A NUMERICAL STUDY OF CROPLAND-ATMOSPHERE FEEDBACKS BY INCORPORATING A CROP GROWTH MODULE IN THE WRF MODEL

BY

DEEKSHA RASTOGI

THESIS

Submitted in partial fulfillment of the requirements
for the degree of Master of Science in Atmospheric Sciences
in the Graduate College of the
University of Illinois at Urbana-Champaign, 2012

Urbana, Illinois

Adviser:

Professor Somnath Baidya Roy

ABSTRACT

This study investigates cropland-atmosphere feedbacks in the Midwestern United States. Growing crops impact local climate during the growing season by influencing heat, moisture and momentum exchange between the land and the atmosphere. These changes in turn affect the crop growth, thus completing a feedback loop. A computationally efficient modeling tool has been specifically developed to study these feedbacks. A vegetation module derived from a crop growth model SUCROS has been incorporated in the Weather Research Forecasting (WRF) model. This coupled model has the capability to explore cropland-atmosphere feedbacks at a high spatial resolution at mesoscale. Results from soybean fields in Nebraska and Illinois show that the crop growth depends directly on temperature, incoming shortwave radiation and precipitation. As the crops grow, they affect energy partitioning between sensible and latent heat leading to a change in the cloud cover and consequently changing incoming shortwave radiation, air temperature and precipitation. An increase in cloud cover reduces incoming shortwave radiation and hence photosynthesis, exerting a negative feedback. However, an increase in precipitation reduces water stress and promotes growth, resulting in a positive feedback. The net impact on crop growth is a nonlinear combination of these feedbacks.

To my parents

ACKNOWLEDGEMENTS

I would like to express my sincere gratitude to my adviser Prof. Somnath Baidya Roy for providing me the opportunity to work on this project. His guidance helped me a lot throughout my research and in writing this thesis. This project would not have been successful without his encouragement and motivation.

I would like to extend my gratitude to the faculty members of the Department of Atmospheric Sciences for teaching the courses, which helped me a lot in developing a strong foundation for this project. I am also very thankful to fellow graduate students for their help. Finally, I want to thank my family and friends for their constant support and inspiration.

This study was supported by National Science Foundation (NSF) grant ATM 08-36756. I am extremely thankful to NSF for funding this project.

TABLE OF CONTENT

LIST OF FIGURES

Figure Page

LIST OF FIGURES (Continued)

Figure Page

LIST OF FIGURES (Continued)

Figure Page

LIST OF FIGURES (Continued)

Figure Page

LIST OF TABLES

CHAPTER 1

INTRODUCTION

Dynamic land surface characteristics, such as vegetation cover, and the surrounding climate interact in a non-linear manner. Changes in atmospheric variables such as moisture, cloud cover, precipitation, temperature, sensible heat flux and latent heat flux amongst others significantly affect vegetation growth. Vegetation growth in turn, directly affects these atmospheric drivers. These two-way interactions are known as atmosphere-vegetation interactions.

Atmosphere-vegetation interactions take place at multiple spatial and temporal scales (Brunsell & Aderson, 2011). At local scale vegetation-atmosphere interactions directly affect the microclimate. For instance, as plants grow they alter earth's surface properties by increasing surface roughness, and increasing evapotranspiration. As evapotranspiration increases, the latent heat flux increases while the sensible heat flux and temperature decrease. As latent heat flux increases, atmospheric moisture increases which results in an increase in cloud cover and precipitation. Increase in cloud cover decreases incoming shortwave radiation reaching the surface reducing photosynthetically active radiation available to plants, therefore photosynthesis is reduced and vegetation growth decreases, ultimately completing the negative feedback loop. Similar to the stated negative feedback loop is a positive feedback loop. Reduction in incoming shortwave radiation due to an increase in cloud cover reduces soil moisture evaporation, increasing the water available to the vegetation, thus increasing plant growth. Increase in precipitation also increases moisture availability and hence increases growth. Decrease in temperature decreases respiratory losses and increases available moisture leading to an increase in growth and also contributing to the positive feedback. A schematic diagram of this feedback

loop is provided in fig. 1.1. Changes in vegetation lead to changes in the distribution of atmospheric energy and the water budget and at the same time changes in atmospheric energy balance and water budget exert a feedback on the plants. The vegetation-atmosphere interaction is a consequence of the non-linear combination of all these processes.

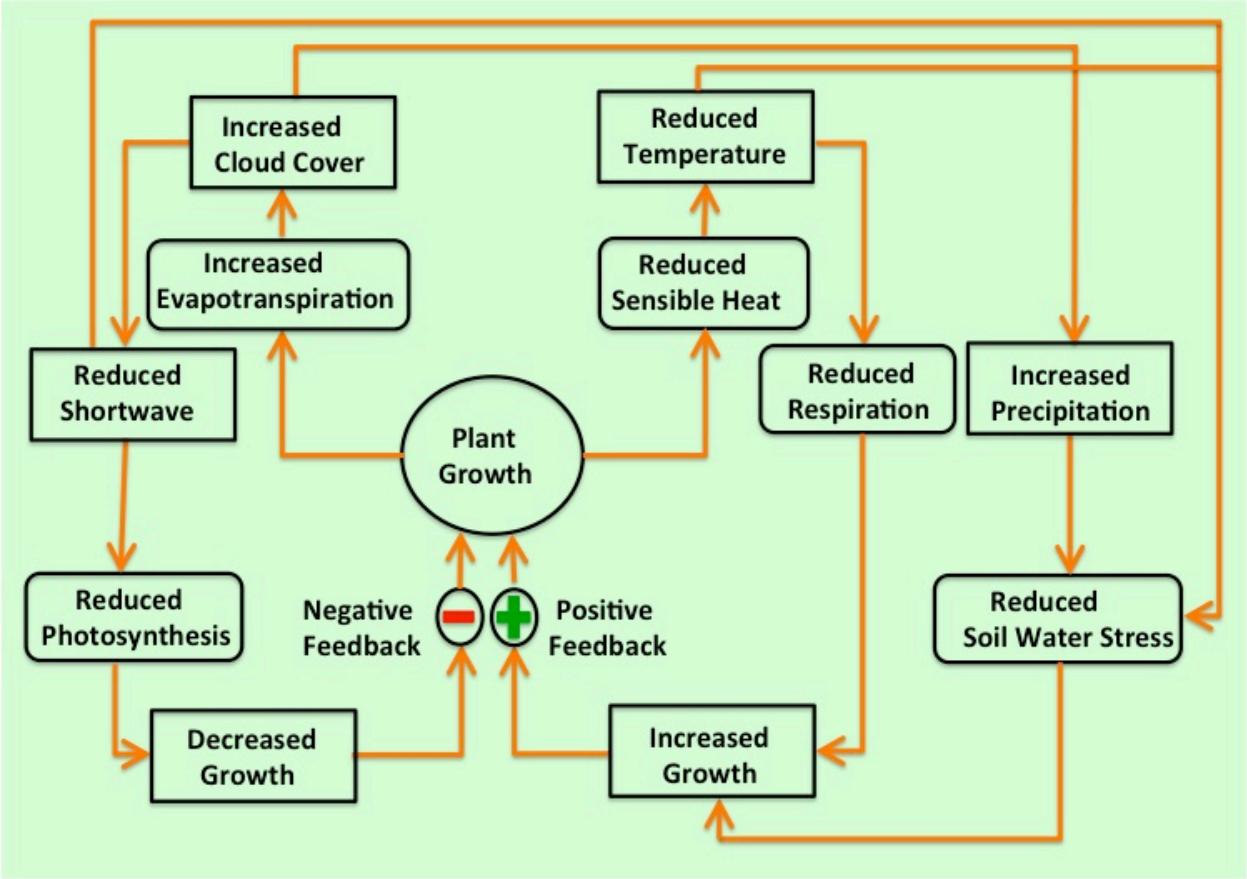

Figure 1.1. A description of vegetation-atmosphere feedback loop.

Most studies related to vegetation-climate interactions either use a fixed vegetation parameter to study the impact of vegetation on the climate or force a vegetation model with results from a climate model to study the effect of climate on vegetation. They do not take into account the affect of dynamic vegetation on climate and the response of climate on the vegetation. However, as mentioned above the changes in land surface properties may also have

an impact on climate, which makes it important to incorporate dynamic vegetation in the climate models.

A few studies have explored this non-linear nature of vegetation-atmosphere interactions at global scale and have suggested that incorporating interactive vegetation improves the simulation of various fluxes in Global Climate models (GCMs). For example, Henderson-Sellers and McGuffie (1995) performed preliminary experiments to test the behavior of a GCM with imposed dynamic changes in vegetation. 11 vegetation types were incorporated in a version of the NCAR Community Climate Model and it was observed that interactive vegetation affects climate directly by changing evaporation. A vegetation model was incorporated in a GCM, GENESIS (version 2) to study these atmosphere-biosphere interactions (Foley et. al.1998). Another dynamic global vegetation model TRIFFID was added to Hadley Centre's coupled global climate model (Cox 2001). In another study Atmosphere-Vegetation Interaction Model (AVIM) was coupled to IAP/LASG GOALS GCM to study these two-way interactions (Dan et al. 2005). Snyder et al. (2004) used Integrated Biosphere Simulator (IBIS) coupled to Community Climate Model version 3 (CCM3) to study the effect of tropical deforestation on regional climate in Africa. Krinner et al. (2005) developed a dynamic global vegetation model ORCHIDEE with the capability to simulate terrestrial carbon cycle as well as changes in vegetation with changes in atmosphere and climate. Bonan et al. (2003) coupled Lund-Potsdam-Jena (LPJ), a dynamic global vegetation model with the National Center for Atmospheric Research (NCAR) land surface model to be used in the Community Climate System Model to understand the feedback of vegetation on the climate. Osborne et al. (2007) analyzed the crop-climate interactions by coupling a crop model to Hadley Centre Atmospheric Model version 3 another GCM. Zeng et al. (2007) coupled atmosphere-vegetation interaction model (AVIM) with

a high resolution GCM SAMIL_R42L9 and on comparing the results with the observations found that the two-way coupled model simulated atmospheric fluxes better than a one way coupled model R42_SSIB. Sato et al. (2007) developed Spatially Explicit Individual-Based Dynamic Global Vegetation Model (SEIB-DGVM) with an additional capability to simulate the interactions among individual trees.

A few studies have also been conducted using regional climate models. For example, Regional Atmospheric Modeling System (RAMS) was coupled with an ecosystem modeling system CENTURY to investigate two-way atmosphere-biosphere interactions. The coupled model used a weekly time step to study these feedbacks (Lu et al. 2001). Shin et al. (2006) studied the effect of changing land surface properties on surface fluxes by coupling Florida State University (FSU) regional spectral model with NCAR Community Land Model, version 2. They also compared the performance of the coupled model with a model, which used simple land surface scheme and observed that the coupling improves the simulation of various atmospheric fluxes in the warm season simulation. This study was conducted at 20 km horizontal resolution over the southeastern United States. In another study, experiments were conducted over the central United States at a resolution of 32 km. It was found that adding an interactive canopy model and a simple ground water model to WRF model improves the simulated summer precipitation over this region (Jiang et al., 2009). Kumar et al. (2011) found that incorporating a photosynthesis-based Gas-exchange Evapotranspiration Model (GEM) into NOAH land surface model improves the simulation of surface fluxes.

In some studies a dynamic vegetation model was added to improve land surface schemes of atmosphere-land surface models, which were used to explore atmosphere-vegetation interactions. The atmosphere-vegetation interaction model (AVIM) was used to simulate annual

variations in surface fluxes. AVIM was based on a physical process mode, plant growth mode and vegetation dynamic parameter mode (Ji 1995). Tsvetsinskaya et al. (2001) studied the effect of crop growth on atmospheric fluxes at a scale of 90 km atmospheric grid cell by incorporating CERES-Maize version 3.0, a plant growth model into Biosphere-Atmosphere Transfer Scheme (BATS). In another study, a dynamic vegetation model was coupled with soil-vegetation-atmosphere transfer scheme (SVAT) (Arora, 2002). Chen et al. (2011) developed BATS-CERES coupled model by incorporating CERES version 3.0 for wheat, maize and rice in BATS. They evaluated the effect of crop growth on surface fluxes over china at a 60 km horizontal resolution. Van Den Hoof et al. (2010) incorporated a dynamic growth model, SUCROS in a land surface model JULES, and found that it significantly improves the performance of the land surface model and captures the variability in growth over croplands in Europe.

It has been well established from the above studies that incorporating dynamic vegetation in climate models improves their performance. However, most of these studies focus on the interactions at large spatial scale. They mostly investigate the vegetation-atmosphere feedbacks at global scale while the studies, which analyze these feedbacks at regional scale are few and are at comparatively coarser horizontal resolution. Due to the absence of dynamic vegetation, most of the current mesoscale models are not capable of capturing these feedbacks. The complex nature of land surface and vegetation distribution makes it important to analyze these feedbacks on regional scale at a high resolution. Moreover it is important to study these interactions over the croplands but only a very few mesoscale models focus on two-way crop-climate interactions. A complete understanding of the effect of climate on crops can be established by interactively coupled climate-crop model (Betts 2005).

The purpose of this study is to understand the complete feedback loop between climate and crops at regional scale at a high spatial resolution. A computationally efficient modeling tool named WRF-CROP has been specifically designed to explore these crop-climate interactions. A vegetation module has been dynamically incorporated in the regional model the Weather Research Forecasting model (WRF) (Skamarock et al., 2008). This vegetation module has been derived from Simple and Universal Crop Growth Simulator (SUCROS) (Goudriaan & Van Laar 1994), a plant growth model. The vegetation module has been calibrated for soybean crop at two sites in the Midwestern United States. In the next two chapters, a description of the models, coupling procedure and sensitivity studies is provided. Chapter 4 contains the comparison of simulated atmospheric fluxes and results between WRF and WRF-CROP coupled model.

CHAPTER 2

SUCROS: CROP GROWTH MODEL

This chapter focuses on a crop growth model, which is based on the Simple and Universal Crop Growth Simulator (SUCROS) (Goudriaan & Van Laar 1994). The crop growth model is capable of simulating a forcing-response relation between the atmosphere and the crop growth. It simulates the effect of atmosphere on the crop growth. In the first section of this chapter, the structure of SUCROS is described, and in the second and the third section, control scenario experiments and sensitivity studies conducted with it are presented.

2.1 Description of SUCROS

SUCROS is a mechanistic model that computes crop growth on the basis of various plant processes and environmental conditions. First, it calculates carbon dioxide assimilation by photosynthesis as a function of temperature, radiation, moisture and leaf area index (LAI). A part of assimilated carbon is used to maintain plant respiration and the remaining part is partitioned among roots, leaves and shoots depending upon the development stage of the plant. LAI is calculated depending on the development stage, accumulated biomass, and environmental factors. At the juvenile stage, LAI is calculated as an exponential function of temperature. In the mature stage it also depends on accumulated biomass and death due to ageing and self-shading. Root depth is directly affected by soil temperature and moisture and it increases until the soil moisture falls below the wilting point or when it reaches a maximum predefined depth. A detailed description of the model can be found in Goudriaan and Van Laar (1994), therefore only a brief description is provided in the following section. A schematic diagram of the crop growth model is provided in Figure 2.1.

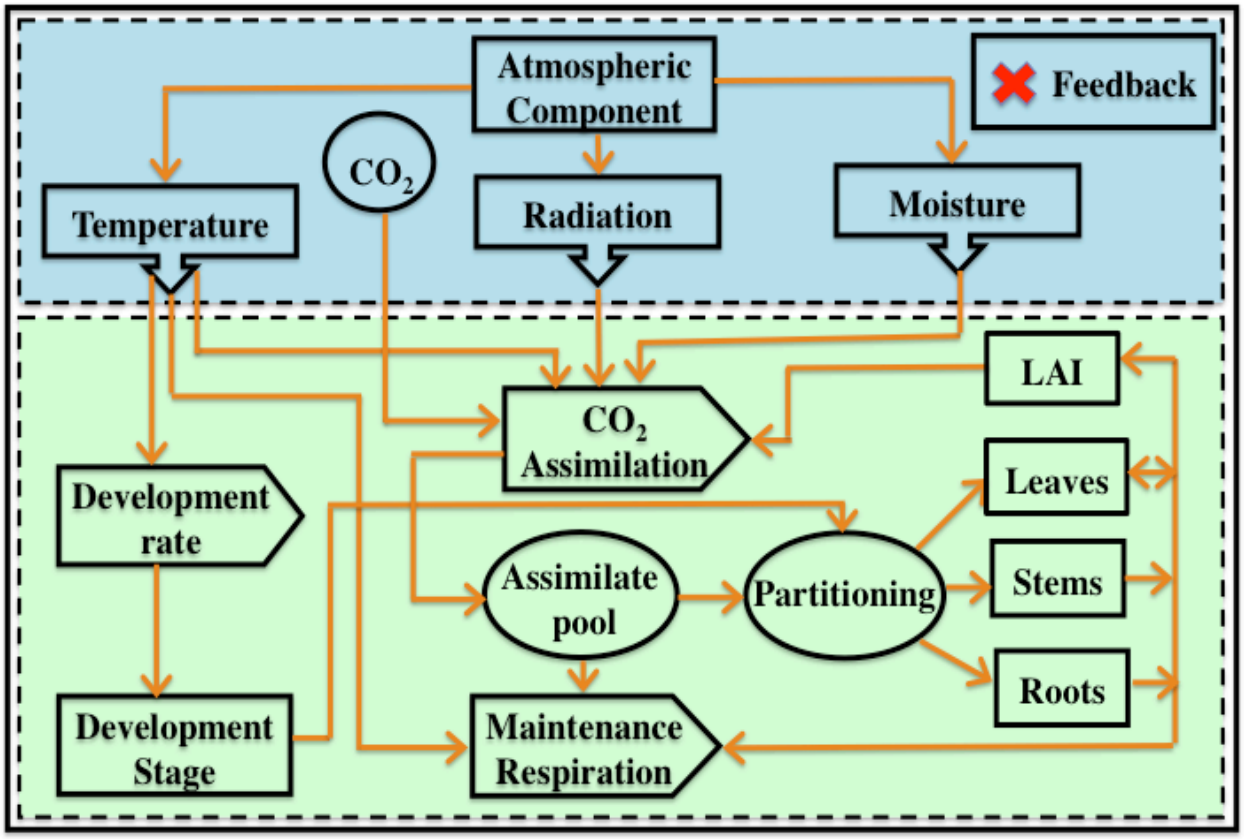

Figure 2.1. A schematic diagram of the crop growth model.

2.1.1 Leaf CO_2 Assimilation

Leaf CO_2 assimilation ($a_{\max}$, g CO_2 m^{-2} leaf s^{-1}) is calculated as a function of its maximum rate at light saturation (a_p, g CO2 m^{-2} leaf s^{-1}), temperature effect, the effect of ageing (a_{dvs}) and emergence of seedling (e) (eq. 2.1). The temperature effect (a_{tmp}) is calculated as the function of averaged daily temperature. The assimilation capacity of full-grown leaves, a_p, varies with crop species. The factor a_{dvs} that accounts for the effect of ageing is a function of the development stage.

$$a_{\max} = a_p * a_{tmp} * a_{dvs} * e \qquad (2.1)$$

2.1.2 Daily Gross CO_2 Assimilation

Daily Gross CO_2 assimilation calculation is based on the photosynthetically active radiation (PAR) absorbed by the canopy. Instantaneous carbon assimilations over and within the canopy are calculated using direct and diffused radiation. A Gaussian integration method is then used to integrate these instantaneous rates to calculate daily gross assimilation (D_a)(Goudriaan & Van Laar, 1994).

Absorbed fluxes per unit leaf area: diffuse flux (V_{sdf} , J m^{-2} leaf s^{-1}), total direct flux (V_{st} , J m^{-2} leaf s^{-1}) and direct component (V_{sd} , J m^{-2} leaf s^{-1}) of direct flux:

$$V_{sdf} = (1 - R_{fh}) * P_{df} * K_{df} * \exp(-K_{df} * L_c) \qquad (2.2)$$

$$V_{st} = (1 - R_{fs}) * P_{dr} * K_{drt} * \exp(-K_{drt} * L_c) \qquad (2.3)$$

$$V_{sd} = (1 - s) * P_{dr} * K_{bl} * \exp(-K_{bl} * L_c) \qquad (2.4)$$

Absorbed flux (V_{sshd} , J m^{-2} leaf s^{-1}) for shaded leaves and assimilation of shaded leaves**:**

$$V_{sshd} = V_{sdf} + V_{st} - V_{sd} \qquad (2.5)$$

$$f_{grsh} = a_{\max} * (1 - \exp(-V_{sshd} * e_{ff} / a_{\max})) \qquad a_{\max} > 0 \qquad (2.6)$$

$$f_{grsh} = 0 \qquad a_{\max} \le 0 \qquad (2.7)$$

Direct flux absorbed by leaves perpendicular on direct beam (V_{pp} , J m^{-2} leaf s^{-1}) and assimilation of sunlit leaf area (V_{sun} , J m^{-2} leaf s^{-1}):

$$V_{pp} = (1 - s) * P_{dr} s_b \qquad (2.8)$$

$$V_{sun} = V_{sshd} + \sum V_{pp} * X_{gauss} \qquad (2.9)$$

$$f_{grs} = a_{\max} * (1 - \exp(-V_{sun} * e_{ff} / a_{\max})) \qquad a_{\max} > 0 \qquad (2.10)$$

$$f_{grs} = 0 \qquad a_{\max} \le 0 \quad (2.11)$$

$$f_{grsun} = \sum f_{grs} W_{gauss} \quad (2.12)$$

Fraction sunlit leaf area (f_{slla}) and local assimilation rate (f_{gl}):

$$f_{sll} = c_f * \exp(-K_{bl} * L_c) \quad (2.13)$$

$$f_{gl} = f_{sll} * f_{grsun} + (1 - f_{sll}) * f_{grsh} \quad (2.14)$$

Integration of local assimilation rate to canopy assimilation (f_{gros}):

$$f_{gros} = \sum f_{gl} W_{gauss} \quad (2.15)$$

Integration of assimilation rate to a daily total (D_a , g CO_2 m^{-2} ground d^{-1}):

$$D_t = \sum f_{gros} W_{gauss} \quad (2.16)$$

$$D_a = D_t * d_l * 3600 \quad (2.17)$$

2.1.3 Carbohydrate Production

The assimilated CO_2 is converted to carbohydrates (CH_2O), denoted here as C using the eq. 2.18.

$$C = D_a * P * 30.0 / 44.0 \quad (2.18)$$

2.1.4 Maintenance Respiration

A part of carbohydrate produced is used for maintaining respiration requirements of various plant organs (leaves, stems, roots and storage organs). Fixed coefficients are used to calculate these requirements. The cost of maintenance increases with increasing temperature. The effect of temperature is taken into account by using t_{eff} . The value of t_{eff} doubles for every 10ºC rise in temperature. The cost of maintenance respiration decreases with ageing of plants due to reduced metabolic activity. The factor, M_{dvs} accounts for the effect of ageing. The

maintenance respiration rate of crop (M , g CH_2O m^{-2} d^{-1}) is calculated as the product of crop's maintenance respiration rate at reference temperature (M_r , g CH_2O m^{-2} d^{-1}), temperature effect, effect of ageing, and emergence of seedlings (eq. 2.19)

$$M = M_r * t_{eff} * M_{dvs} * e \tag{2.19}$$

$$M_r = M_{lv} * W_{lv} + M_{st} * W_{st} + M_{rt} * W_{rt} + M_{so} * W_{so} \tag{2.20}$$

2.1.5 Plant Organ Development & Partitioning

The assimilate requirement (a_{srq}) for conversion of carbohydrate to dry matter is calculated as the weighted mean of assimilate requirement for different plant organs (eq. 2.21). For a particular plant organ, the assimilate requirement depends on its chemical composition. The growth rates of different plant organs are calculated as the product of overall growth rate (G_r) and fractions allocated to various organs (eq. 2.23, 2.24, 2.25 & 2.26). Translocation rate (T , g DM m^{-2} d^{-1}) depends on crop development stage (eq. 2.27 & eq. 2.28) and is calculated as a function of the development rate of the crop.

Assimilate requirement (a_{srq} , g CH_2O g^{-1} DM):

$$a_{srq} = f_{sh} * (a_{lv} * f_{lv} + a_{st} * f_{st} + a_{so} * f_{so}) + a_{rt} * f_{rt} \tag{2.21}$$

Gross growth rate (G_r , g DM m^{-2} ground d^{-1}):

$$G_r = (C - M + (c * T * f_{cst} * 30.0 / 12.0)) / a_{srq} \tag{2.22}$$

Dry matter growth rate of roots, (G_{rt} , g DM m^{-2} ground d^{-1})

$$G_{rt} = f_{rt} * G_r \tag{2.23}$$

Dry matter growth rate of roots, (G_{lv} , g DM m^{-2} ground d^{-1})

$$G_{lv} = f_{rt} * f_{sh} * G_r \tag{2.24}$$

Dry matter growth rate of roots, (G_{st} , g DM m^{-2} ground d^{-1})

$$G_{st} = f_{st} * f_{sh} * G_r - T \qquad (2.25)$$

Dry matter growth rate of roots, (G_{so} , g DM m^{-2} ground d^{-1})

$$G_{so} = f_{so} * f_{sh} * G_r \qquad (2.26)$$

Translocation rate (T , g DM m^{-2} d^{-1})

$$T = 0.0 \qquad d_s - 1 < 0.0 \qquad (2.27)$$

$$T = W_{st} * d_r * f_{rtrl} \qquad d_s - 1 \geq 0.0 \qquad (2.28)$$

2.1.6 Leaf Development

Growth rate depends on phenological development stage of plants. Growth rate is zero before the emergence of the seedlings (eq. 2.29) and after the emergence, growth rate is influenced by temperature and light intensity (eq. 2.30). The growth rate in mature stage is calculated as a product of simulated increase in leaf weight (G_{lv}) and the specific leaf area (s_a) of new leaves (eq. 2.31). The senescence rate (D_l) is calculated from relative death rate D_r (eq. 2.34), which is a maximum of death rate due to ageing (D_{rdv}) and due to self shading of leaves (D_{rss}) (eq. 2.32). Leaf area index (LAI) is calculated as a difference between growth rate (G) and senescence rate (D_l) (eq. 2.34 & 2.35).

Growth before seedling emergence:

$$G = 0 \qquad d < d_{em} \qquad (2.29)$$

Growth during juvenile stage:

$$G = L * \left(\exp\left(r * dt_{eff} * t\right) - 1.0\right) / t \qquad D_s < 0.3 \,\&\, L < 0.75 \qquad (2.30)$$

Growth during mature stage:

$$G = s_a * G_{lv} \quad (2.31)$$

Death rate:

$$D_r = \max\left(D_{rdv}, D_{rss}\right) \quad (2.32)$$

$$D_l = L * D_r \quad (2.33)$$

Net growth:

$$R_l = G - D_l \quad (2.34)$$

Leaf Area Index :

$$L = L + R_l * t \quad (2.35)$$

2.1.7 Root Growth

Rate of root growth depends primarily on soil temperature and varies slightly with root biomass. The roots in the model grow until soil moisture reduces below wilting point or if the root depth reaches a predefined maximum limit.

Rate of Root elongation (e_{rt} , mm/d):

$$e_{rt} = e_{rtc} * w_{sert} * a_{tmp} \quad (2.36)$$

Rooted Depth (z_{rt} , mm):

$$z_{rt} = z_{rt} + e_{rt} * d_t \quad (2.37)$$

2.1.8 Atmospheric Component

In this section, the atmospheric component of the crop growth model has been described. The model is forced with daily averaged data of incoming shortwave radiation, maximum and minimum temperature, vapor pressure, wind speed and precipitation. The plant canopy intercepts a part of precipitation, another part becomes runoff and the remaining portion infiltrates into the soil. Infiltrated water is redistributed among the four vertical soil compartments ($T_{l1}, T_{l2}, T_{l3}, T_{l4}$).

Any excess water in the deepest layer is drained out. If the water cannot be drained, it fills up the soil layers forming a perched water table first, saturating the deepest layer. After the entire soil profile is saturated, water flows on the surface accounting for waterlogged condition.

$$I = \min(R, i * L) \tag{2.38}$$

$$R_{off} = \max(0, 0.15 * (R - I - 10), R - I - (w_{st1} * T_{l1} - w_{l1}) / 2 * d_t \tag{2.39}$$

$$I_f = R - I - R_{off} \tag{2.40}$$

If sufficient water is available, water uptake takes place at the rate of potential evapotranspiration. Penman-Monteith equation is used to calculate potential evapotranspiration (p_{et}). Penman potential evapotranspiration is calculated as the sum of evapotranspiration due to radiation (e_{rad}) and due to the drying power of air (e_d). Under insufficient moisture availability, water uptake takes place at actual evapotranspiration rate. Actual transpiration is calculated as the sum of water uptake from each soil compartment. Actual evaporation is calculated depending upon the rain on a particular day. For the days it rains, actual evaporation rate is set equal to potential evaporation rate and on the days without rain it has a value below potential evaporation rate. The effect of water stress on water uptake, CO2 assimilation and carbohydrate partitioning is taken into account using different factors calculated as a function of actual and potential evapotranspiration.

Radiation Term:

$$e_{rad} = (1 / l) * (S / (S + p)) * n_{rad} \tag{2.41}$$

Drying Power Term:

$$e_d = d_{rp} / (S + p) \tag{2.42}$$

Potential Evaporation:

$$p_e = \exp(-0.5 * L) * (e_{rad} + e_d) \tag{2.43}$$

Potential Transpiration:

$$p_t = (1 - \exp(-0.5 * L)) * e_{rad} + e_d * \min(2.0, L) - 0.5 * I \tag{2.44}$$

Potential Evapotranspiration:

$$p_{et} = p_e + p_t \tag{2.45}$$

2.2 Control Scenario Experiment

The crop growth was simulated over an Ameriflux site in Nebraska. The experiment was conducted for soybean crop for the 2006-growing season. The model was calibrated for the soybean crop (Table 2.1). The model was forced with the daily atmospheric data obtained from the Ameriflux website (http://public.ornl.gov/ameriflux/) for US-Ne3 site in Nebraska (Latitude: 41.17 Longitude: -96.43) (Figure 2.2). The modeled LAI was found comparable to the observed LAI also obtained from the Ameriflux website (Figure 2.3).

Figure 2.2 Location of Nebraska site.

Parameter	Value	Source
a_p	0.0009636 g CO_2 m^{-2} leaf s^{-1}	a
e	0 before emergence 1 after emergence	b
e_{ff}	12.5 X 10^{-6} g CO_2 / J	b
K_{df}	0.60 m^2 ground ha^{-1} leaf	b
s	0.20	b
s_a	0.025 m^2 leaf/g leaf	c
M_{lv}	0.03 g CH_2O g^{-1} DM d^{-1}	b
M_{rt}	0.015 g CH_2O g^{-1} DM d^{-1}	b
M_{st}	0.015 g CH_2O g^{-1} DM d^{-1}	b
M_{so}	0.01 g CH_2O g^{-1} DM d^{-1}	b
W_{lv}	0.5 g m^{-2} (Initial value)	b
W_{rt}	0.8 g m^{-2} (Initial value)	b
W_{so}	0 g m^{-2} (Initial value)	b
W_{st}	0.3 g m^{-2} (Initial value)	b
r	0.009(°C d)$^{-1}$	b
a_{lv}	1.463 g CH_2O g^{-1} DM leaf	b
a_{rt}	1.444 g CH_2O g^{-1} DM leaf	b
a_{st}	1.513 g CH_2O g^{-1} DM leaf	b
a_{so}	1.415 g CH_2O g^{-1} DM leaf	d, e
c	0.947	e
t	1 day	b
i	0.25	b
e_{rtc}	12	b
T_{l1}	200 mm	b
T_{l2}	400 mm	b
T_{l3}	600 mm	b
T_{l4}	800 mm	b

Table 2.1 List of parameters for the crop growth model.

a: Murata, 1992
b: Goudriaan & Van Laar 1994
c: Setiyono et. al, 2008
d: Penning de Vries & van Laar, 1982
e: Penning de Vries et al., 1989

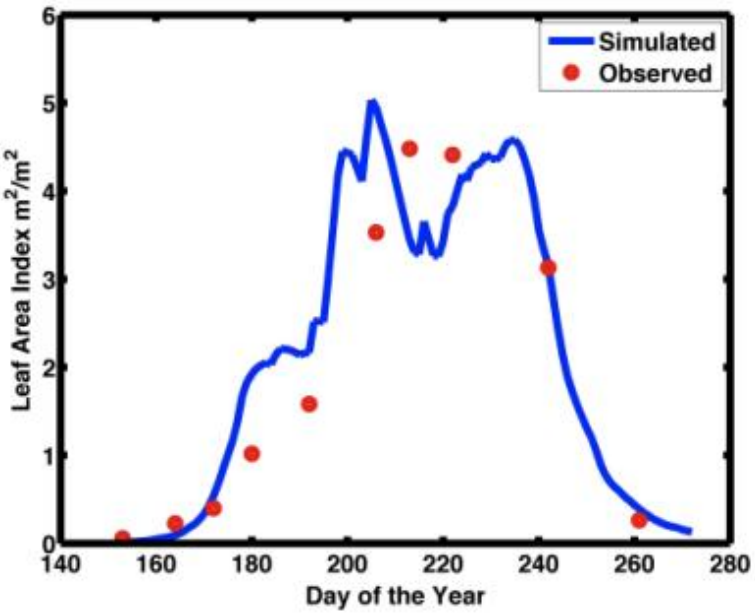

Figure 2.3 Modeled and observed Leaf Area Index over the Nebraska site.

2.3 Sensitivity Study

The crop growth is affected by atmospheric conditions. Leaf area index (LAI) is determined mainly by three environmental factors: temperature, incoming shortwave radiation and moisture. Field experiments such as rainfall exclusion experiment are used to understand the relation between atmospheric variables and growth. Experiments in greenhouse are also conducted to study these relations. However, these experiments are expensive and it takes almost an entire season to complete these experiments. Therefore, I conduced several experiments with the model to analyze the role of these atmospheric variables in simulating crop growth. The model was calibrated over soybean fields in Nebraska for the 2006 growing season. The model was forced with the daily atmospheric data from the Ameriflux US-Ne3 site (Latitude: 41.17 Longitude: -96.43). First, the variables were changed linearly; i.e., one variable was changed at a time while keeping the other variables constant. The variables were then allowed to interact non-linearly by changing more than one variable at a time. A list of all the runs conducted is provided

in Table 2.2 and Table 2.3 but only some of the selected results are presented in the following section.

Single Variable Sensitivity Study				
Variable	*Change w.r.t. Control*	*Time Period*	*Amount Changed*	*No. of Simulations*
Temperature	Increased	Entire Cycle	by 1ºC, 3ºC, 5ºC, 7ºC & 10ºC	15
		Juvenile Stage		
		Mature Stage		
	Decreased	Entire Cycle	by 1ºC, 3ºC, 5ºC, 7ºC & 10ºC	15
		Juvenile Stage		
		Mature Stage		
Precipitation	Increased	Entire Cycle	by 10%, 20%, 50%, 70% & 100%	15
		Juvenile Stage		
		Mature Stage		
	Decreased	Entire Cycle	by 10%, 20%, 50%, 70% & 100%	15
		Juvenile Stage		
		Mature Stage		
Shortwave Radiation	Increased	Entire Cycle	by 10%, 30%, 50%, 55% & 60%	15
		Juvenile Stage		
		Mature Stage		
	Decreased	Entire Cycle	by 10%, 30%, 50%, 55% & 60%	15
		Juvenile Stage		
		Mature Stage		
Soil moisture	Increased/Decreased	Initial moisture	to 0.2,0.25,0.34,04	8
		Entire Cycle	60%, 70%, 80%, 90% & 100% Saturated	5
			Total number of Simulations	103

Table 2.2 List of runs conducted for Linear Sensitivity Study.

Multi-Variable Sensitivity Study			
	Changes in 1st Variable	Changes in 2nd Variable	
Temperature & Precipitation	Temperature increased by 1ºC, 3ºC, 5ºC, 7ºC & 10ºC	Precipitation increased by 10%, 20%, 50%, 70% & 100%	50
		Precipitation decreased by 10%, 20%, 50%, 70% & 100%	
	Temperature decreased by 1ºC, 3ºC, 5ºC, 7ºC & 10ºC	Precipitation increased by 10%, 20%, 50%, 70% & 100%	50
		Precipitation decreased by 10%, 20%, 50%, 70% & 100%	
Precipitation & Radiation	Precipitation increased by 10%, 20%, 50%, 70% & 100%	Radiation increased by 10%, 30%, 50%, 55% & 60%	50
		Radiation decreased by 10%, 30%, 50%, 55% & 60%	
	Precipitation decreased by 10%, 20%, 50%, 70% & 100%	Radiation increased by 10%, 30%, 50%, 55% & 60%	50
		Radiation decreased by 10%, 30%, 50%, 55% & 60%	
Radiation & Temperature	Radiation increased by 10%, 30%, 50%, 55% & 60%	Temperature increased by 1ºC, 3ºC, 5ºC, 7ºC & 10ºC	50
		Temperature decreased by 1ºC, 3ºC, 5ºC, 7ºC & 10ºC	
	Radiation decreased by 10%, 30%, 50%, 55% & 60%	Temperature increased by 1ºC, 3ºC, 5ºC, 7ºC & 10ºC	50
		Temperature decreased by 1ºC, 3ºC, 5ºC, 7ºC & 10ºC	
Total number of Simulations			300

Table 2.3 List of runs conducted for Non-Linear Sensitivity Study.

2.3.1 Single-Variable Sensitivity Study

2.3.1a *Temperature*

Near surface air Temperature is an important factor that affects plant growth. It controls maintenance respiration of plants, soil water evaporation, assimilation and development rate. 1) Maintenance respiration of plants varies directly with the temperature. Increasing temperature increases maintenance respiration, which act to reduce growth. 2) Soil water evaporation also varies directly with the temperature. Increasing temperature increases soil water evaporation, which reduces soil moisture availability and hence decreases growth. 3) Assimilation rate increases with increasing temperature upto a crop dependent threshold temperature, beyond this threshold, assimilation rate decreases. 4) Development rate also increases with increasing temperature until a threshold temperature is met. Above this threshold temperature, development rate does not increase any further. The net effect of increasing temperature is a non-linear combination of these four factors.

Temperature was increased and decreased over an entire season and during different plant growth stages to understand the dependence of plant growth on temperature. Different temperature scenarios for this sensitivity are provided in Figure 2.4.

Temperature was increased by 1, 3, 5, 7 and 10ºC over the entire season (Figure 2.4a). It was observed that the reduction in growth was slow in the beginning and accelerated in the mature stage (Figure 2.5a). Initially, the decrease in growth was slow because of an increase in assimilation and development rate but later on the first two factors; increased plant respiration and increased evaporation dominated reducing the overall growth. Life span of plants was also found to decrease with increasing temperature. This was due to an increase in development rate, which caused plants to grow and die at a faster rate. Increase in temperature in the juvenile stage

(Figure 2.5b) increased growth in that stage. This can be attributed to the fact that growth in the juvenile stage is an exponential function of temperature. However, a decrease in growth was seen in the remaining growth cycle. Temperature was also increased in mature stage but since the results were similar to Figure 2.5a.

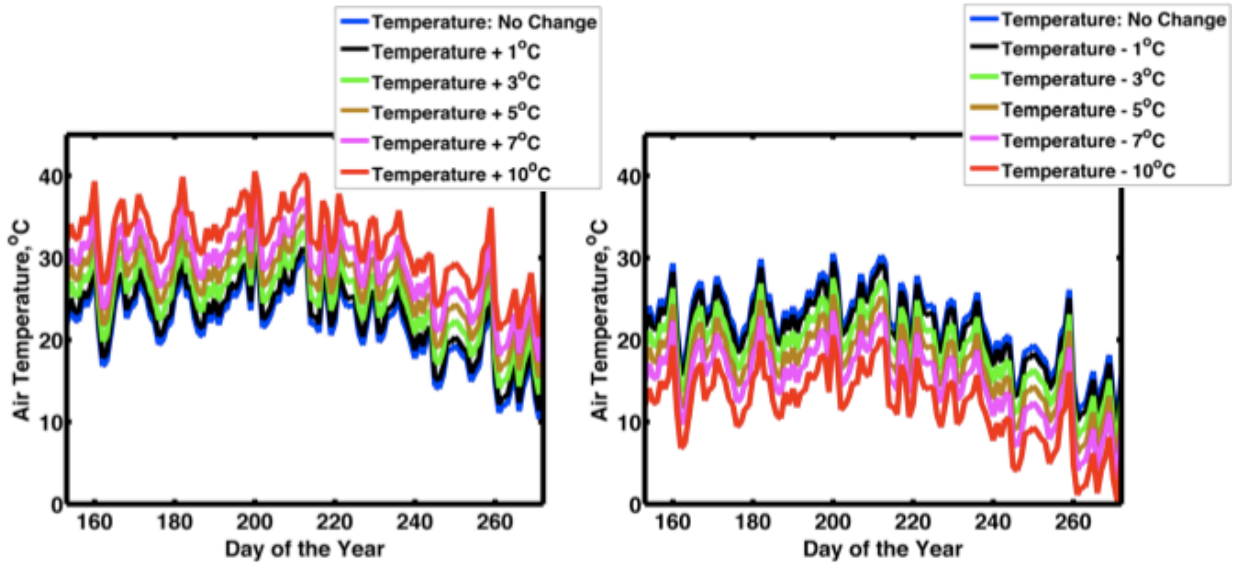

(a) *(b)*

Figure 2.4 Temperature plot for different runs (a) Increase in temperature, (b) Decrease in temperature.

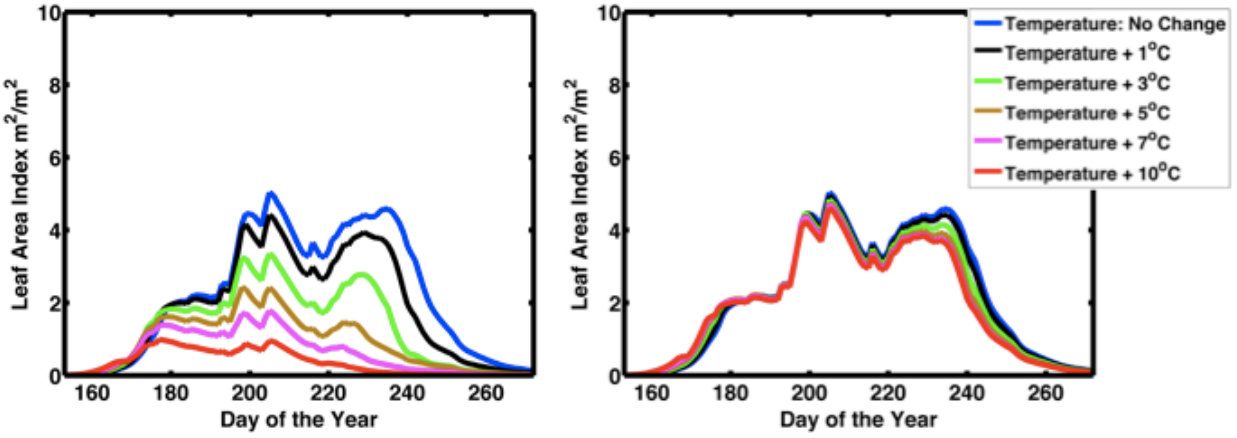

(a) *(b)*

Figure 2.5 Leaf Area Index with increasing temperature (a) over the entire growing season, (b) during the juvenile stage.

Temperature was reduced by 1, 3, 5, 7 and 10°C over the entire season (Figure 2.4b).

Decreased temperature over the entire season decreased growth in the juvenile stage and increased growth over the remaining season. However, a minimum temperature threshold was observed. At a certain lower temperature, soil moisture does not evaporate efficiently leading to an excess of soil moisture. At this temperature, assimilation and development rates are also low which results in limited growth. Growth increased with decreasing temperature in mature stage until a decrease of 7ºC and any decrease beyond 7ºC decreased growth (Figure 2.6a). Life span of plants directly depends on temperature. Decreased temperature reduced development rate leading to an increased life span. On decreasing temperature in juvenile stage (Figure 2.6b), growth was inhibited during this stage, but during remainder of the growing cycle, growth increased. Temperature was also decreased in mature stage and the results were similar to Figure 2.6a.

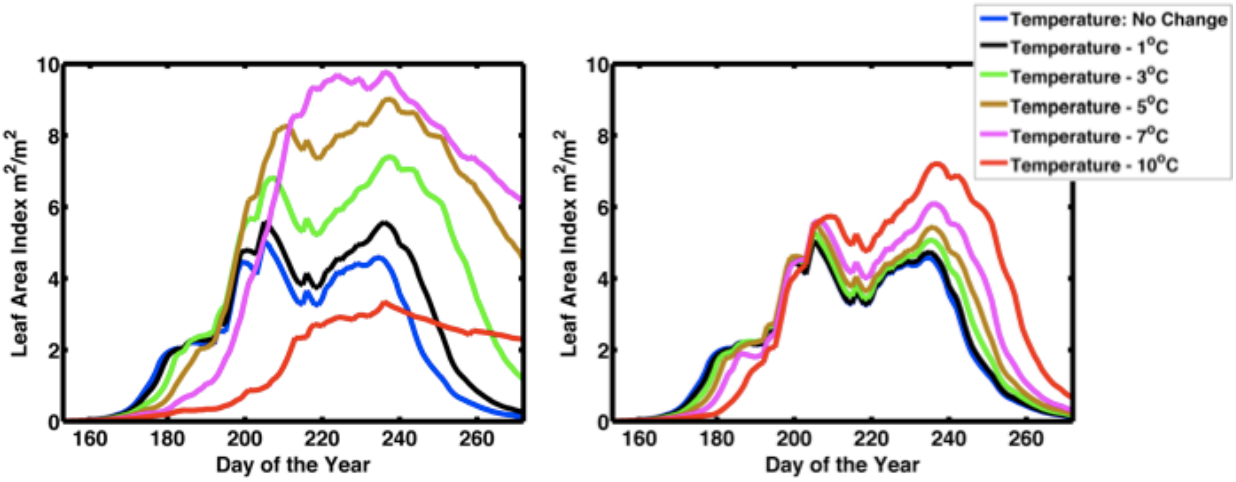

(a) *(b)*

Figure 2.6 Leaf Area Index with decreasing temperature (a) over the entire growing season, (b) during the juvenile stage.

2.3.1b *Moisture*

Soil moisture content is another important factor that controls growth. Increasing soil moisture content increases photosynthesis until a certain threshold value is reached and any

increase in soil moisture beyond that decreases photosynthesis while decreasing soil moisture decreases growth. Soil moisture is controlled by precipitation in the absence of irrigation. In order to test the effect of moisture, precipitation was varied over the region.

Precipitation was increased and decreased over an entire season and during different plant growth stages to understand the dependence of plant growth on soil moisture. Different precipitation scenarios for this sensitivity are provided in Figure 2.7.

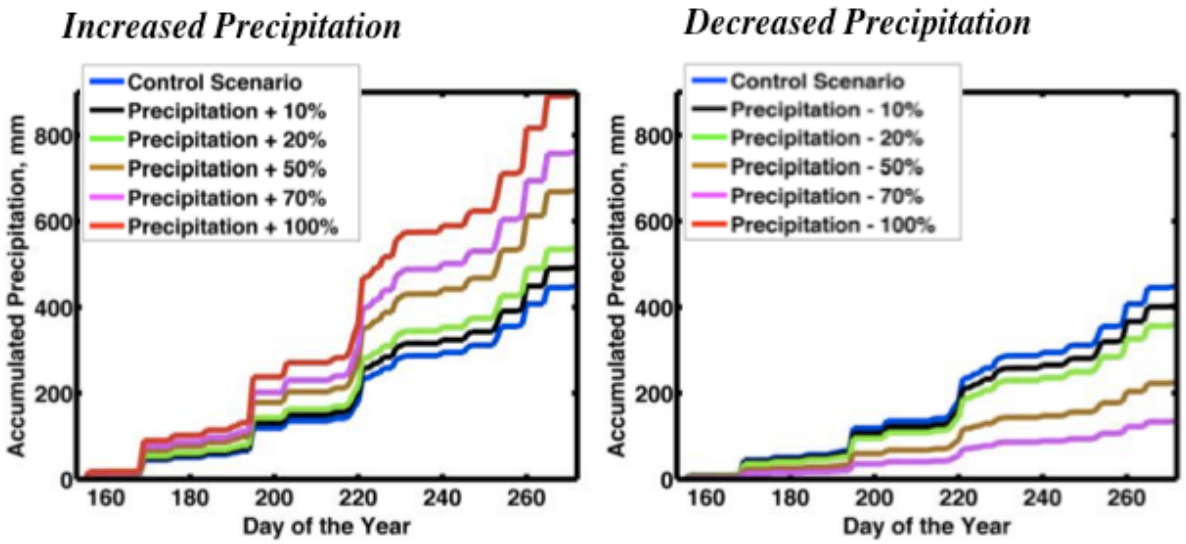

(a) *(b)*

Figure 2.7 Temperature plot for different runs (a) Increase in temperature, (b) Decrease in temperature.

In decreased precipitation scenario (Figure 2.7b), growth was observed to decrease. Figure 2.8a shows the effect of reducing precipitation over the entire season on growth and Figure 2.8b shows the effect of reducing precipitation in juvenile growth stage. Reducing precipitation was observed to reduce growth. Reducing precipitation over the entire season (Figure 2.8a) reduced growth initially at a slow rate and then at a fast rate while decreasing precipitation in the juvenile stage (Figure 2.8b) also reduced growth over the entire growth cycle

but only by a small amount. The results on reducing precipitation in mature stage were similar to Figure 2.8a and are not shown here.

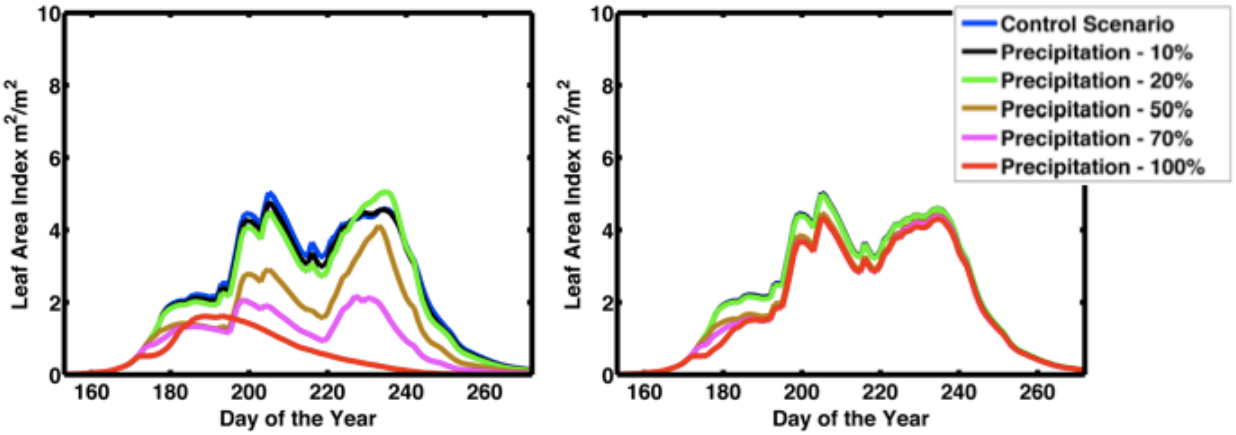

(a) *(b)*

Figure 2.8 Leaf Area Index with decreasing precipitation (a) over the entire growing season, (b) during the juvenile stage.

Increased precipitation over the entire cycle increased growth (Figure 2.9a) but only a small increase was observed with increased precipitation in juvenile stage (Figure 2.9b). The results from increasing precipitation in mature stage were similar to Figure 2.9a and are not shown here.

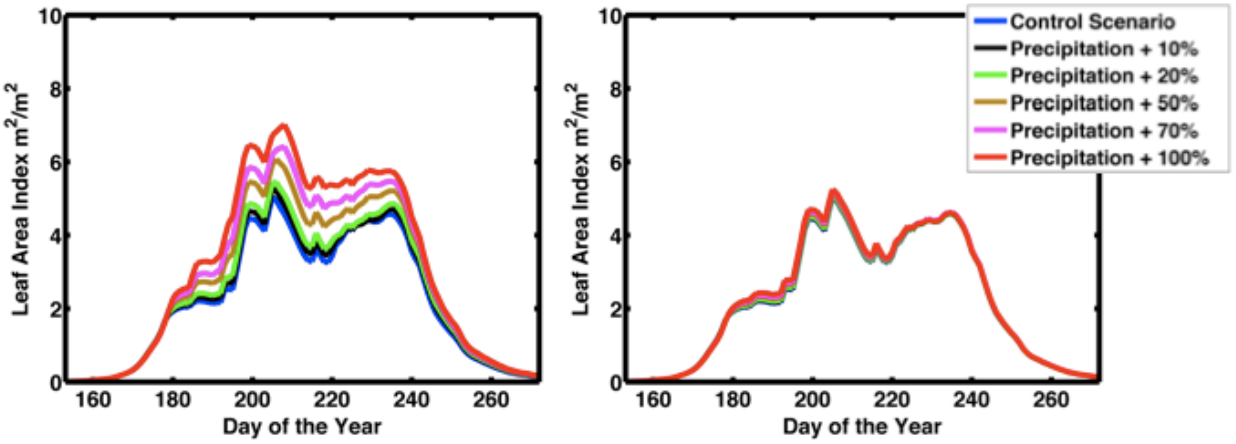

(a) *(b)*

Figure 2.9 Leaf Area Index with decreasing precipitation (a) over the entire growing season, (b) during the juvenile stage.

Soil moisture was changed to further understand the behavior of the model. Initial soil moisture was found to affect the growth over the entire season. In Figure 2.10b, initial soil moisture was varied between 0.2 and 0.4. As the initial soil moisture increased, growth in the mature stage and LAI peak was also observed to increase. In order to understand the threshold soil moisture content beyond which the growth will not increase any more, the soil moisture was changed over the entire season in the model. In Figure 2.10a, soil moisture for the entire growth cycle was maintained at 60%, 70%, 80%, 90% and 100% saturation. The growth and peak LAI increased until the soil was 70% saturated and reduced thereafter.

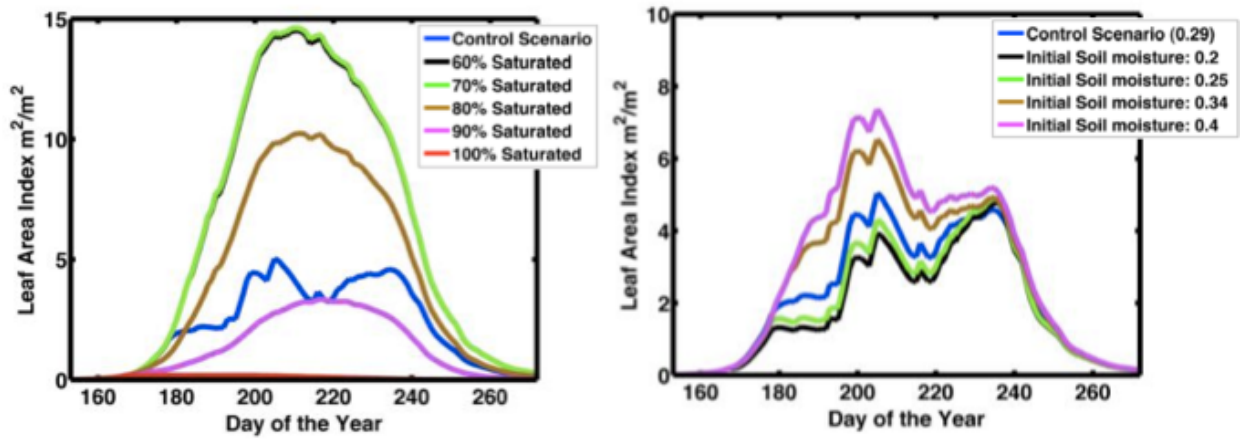

(a) *(b)*

Figure 2.10 Leaf Area Index with changing (a) soil moisture over the entire growing season, (b) initial soil moisture.

Growth was observed to decrease with decreasing moisture content and increase with increasing moisture but after sufficient moisture was available, any further increase in the soil moisture reduced growth. In a completely biophysical environment, plants grow faster and the growth is high if more soil water is available. After a certain point, addition of water does not affect growth anymore, i.e., when LAI maximum is reached.

2.3.1c *Radiation*

Incoming short wave radiation provides photosynthetically active radiation (PAR), a

necessary component for the photosynthetic process. It also controls the soil moisture evaporation. The net result of changing incoming shortwave radiation is a combination of these two factors. Incoming short wave radiation was increased and decreased over an entire season and during different plant growth stages to understand the dependence of plant growth on soil moisture. Different short wave radiation scenarios for this sensitivity are provided in Figure 2.7.

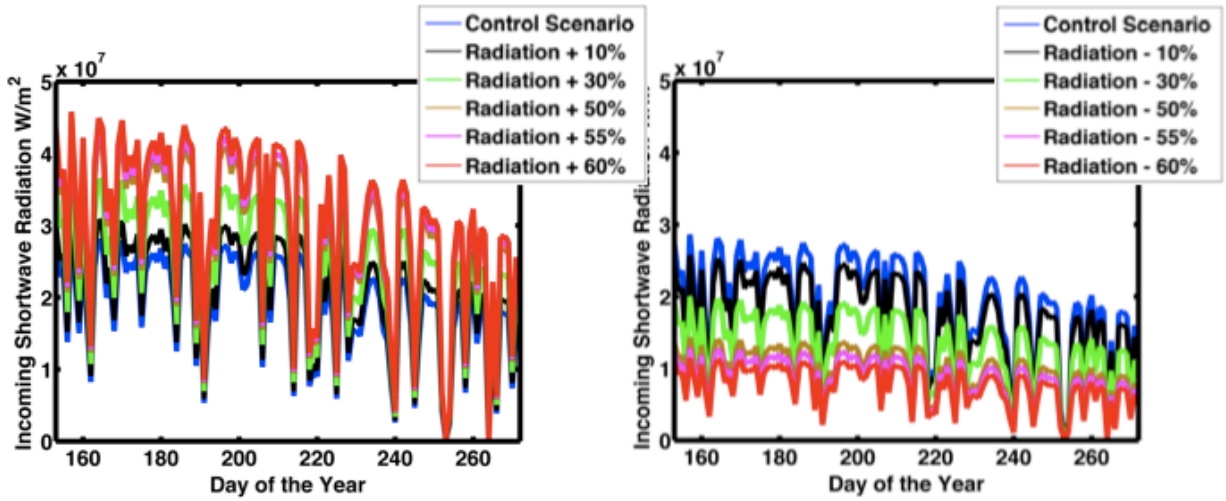

(a) *(b)*

Figure 2.11 Incoming shortwave radiation plot for different runs (a) Increase in temperature, (b) Decrease in temperature.

With small decrease in radiation, growth and LAI peak was seen to increase but any decrease above 30% reduced the growth and LAI peak (Figure 2.12a). With decrease in radiation, soil water evaporation reduces but at the same time photosynthesis also reduces. Initially, due the presence of more moisture, growth increased but after a certain decrease in radiation, reduction in photosynthetic activity dominated over the moisture availability and growth reduced. On the days with low radiations, for instance, on 240th day of the year (Figure 2.11b), growth was observed to depend directly on radiation, a small decrease in radiation did not affect the growth but a higher decrease (> 30%) reduced growth.

Reducing radiation in juvenile stage increased growth but only marginally (Figure 2.12b). A similar study was conducted for the mature stage of plant growth and results were similar to Figure 2.12a.

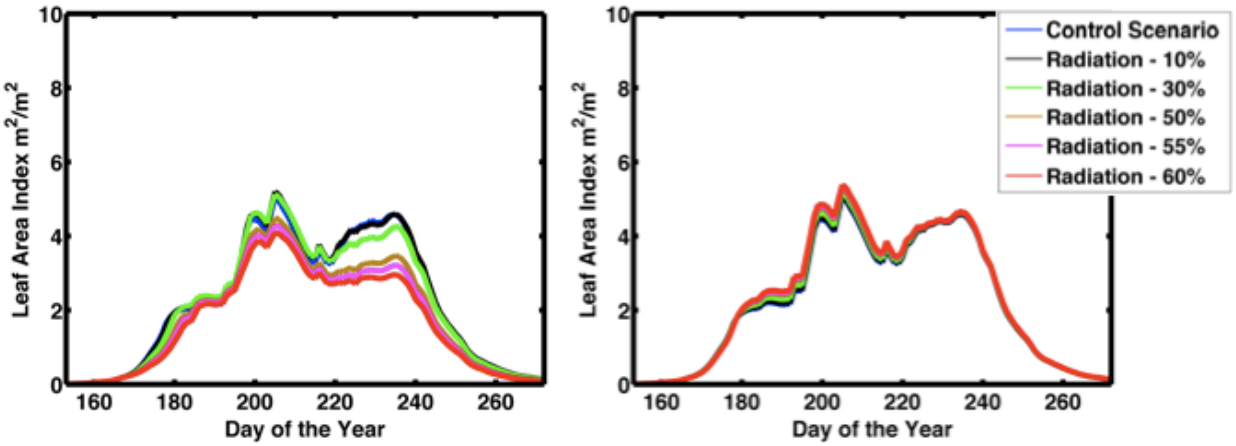

(a) *(b)*

Figure 2.12 Leaf Area Index with decreasing incoming shortwave radiation (a) over the entire growing season, (b) during the juvenile stage.

Increase in radiation over the entire season reduced growth and LAI due to reduced moisture availability. The days when incoming radiation was low, for example on 240th day of the year (Figure 2.11a) increase in radiation was seen to increase the growth as increase in photosynthetic radiation dominated over lower moisture availability. Similarly, when radiation was increased in the juvenile stage (Figure 2.12b), the growth decreased but only by a small amount. The results for mature stage were similar to Figure 2.12a and are not shown here.

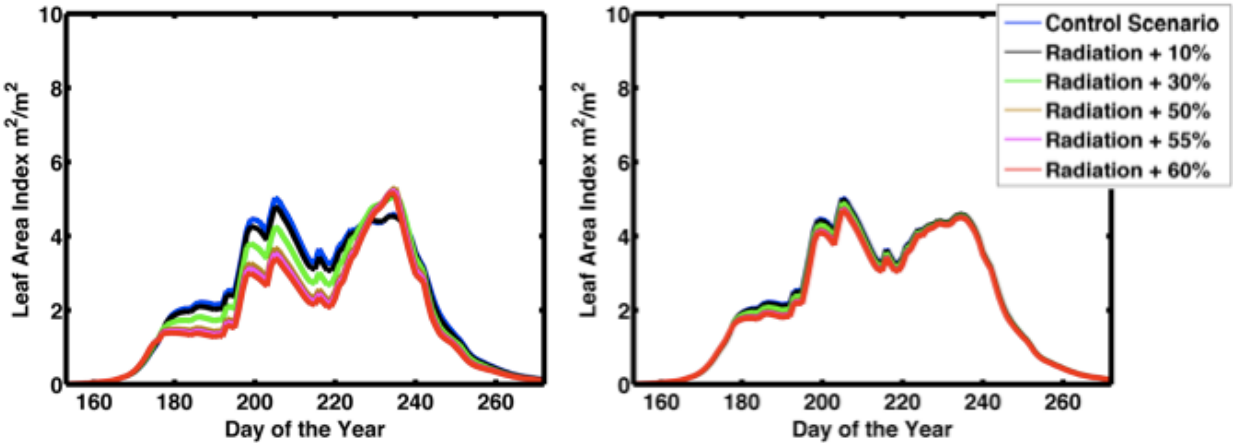

(a) *(b)*

Figure 2.13 Leaf Area Index with decreasing incoming shortwave radiation (a) over the entire growing season, (b) during the juvenile stage.

2.3.2 Multi-Variable Sensitivity Study

2.3.2a *Incoming shortwave and temperature*

The individual effect of temperature and radiation on crop growth has been discussed in the sections 2.3.1a and 2.3.1c respectively. In this section, we changed these two variables simultaneously to study their combined affect on the growth.

(i) Decreased Radiation and Decreased Temperature:

Decreasing both incoming shortwave radiations and temperature reduced soil water evaporation leading to an increased plant growth. However, after sufficient moisture was available any further decrease in radiation or temperature reduced growth. In Figure 2.14a,b and c, incoming shortwave radiation was decreased by 10%, 30% and 60% respectively and in each case temperature was decreased by 1, 3, 5, 7 and 10ºC. When radiation was reduced by 10% (Figure 2.14a), growth increased until temperature was decreased by 7ºC, any decrease in temperature beyond that reduced growth. Decreasing radiation by 30% (Figure 2.14b) decreased this temperature threshold to 5ºC. However, when radiation was decreased by 60% (Figure

2.14c), growth reduced as compared to Figure 2.14a and Figure 2.14b for a particular decrease in temperature due to reduced availability of photosynthetically active radiations.

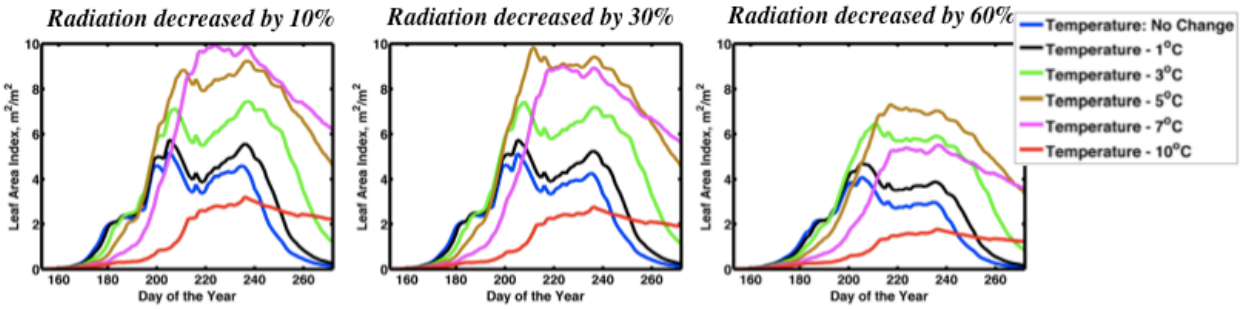

(a) *(b)* *(c)*

Figure 2.14 Leaf Area Index with (a) radiation reduced by 10%, (b) radiation reduced by 30%, (c) radiation reduced by 60%. In each case, temperature was decreased by 1, 3, 5, 7 & 10°C.

(ii) Increased Radiation and Increased Temperature:

Simultaneously increasing radiation and temperature increased soil water evaporation leading to reduced moisture availability. Increased radiation also increased PAR. However, limited moisture supply dominated over abundant availability of PAR, and growth decreased (Figure 2.15).

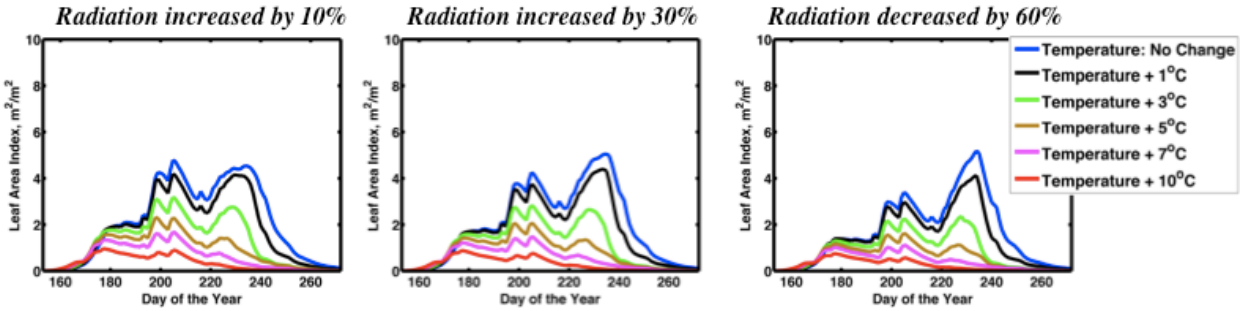

(a) *(b)* *(c)*

Figure 2.15 Leaf Area Index with (a) radiation increased by 10%, (b) radiation increased by 30%, (c) radiation increased by 60%. In each case, temperature was increased by 1, 3, 5, 7 & 10°C.

(iii) Decreased Radiation and Increased Temperature:

Increasing temperature increased soil water evaporation while decreasing radiation decreased it. The effect of increased temperature dominated over decreased incoming radiation leading to insufficient moisture availability and reduced growth (Figure 2.16).

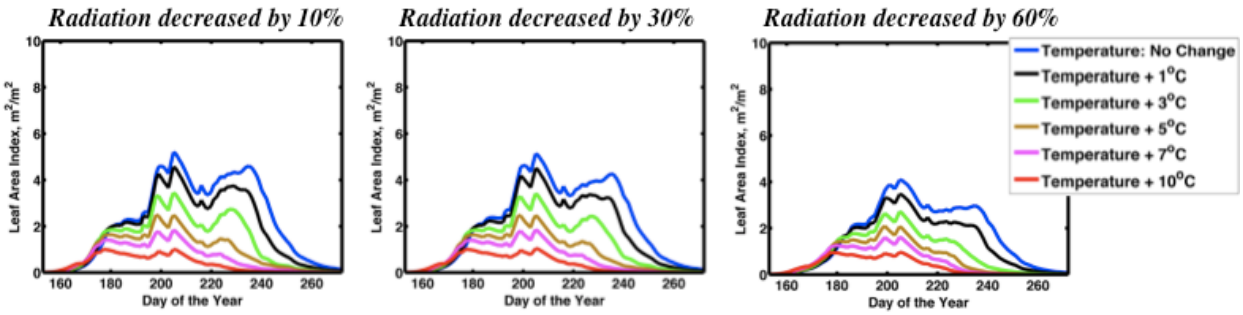

(a) *(b)* *(c)*

Figure 2.16 Leaf Area Index with (a) radiation decreased by 10%, (b) radiation decreased by 30%, (c) radiation decreased by 60%. In each case, temperature was increased by 1, 3, 5, 7 & 10°C.

(iv) Increased Radiation and Decreased Temperature:

Decreasing temperature increased moisture availability but reduced assimilation and development rate. Increased radiation provided abundant PAR but reduced soil moisture content. The net change in growth is a non linear combination of these factors. Independent of the amount of increase in radiation, the growth increased until temperature reduced by 7°C but any decrease in temperature beyond that reduced growth (Figure 2.17). However, for a particular decrease in temperature, the net growth decreased with increased radiation.

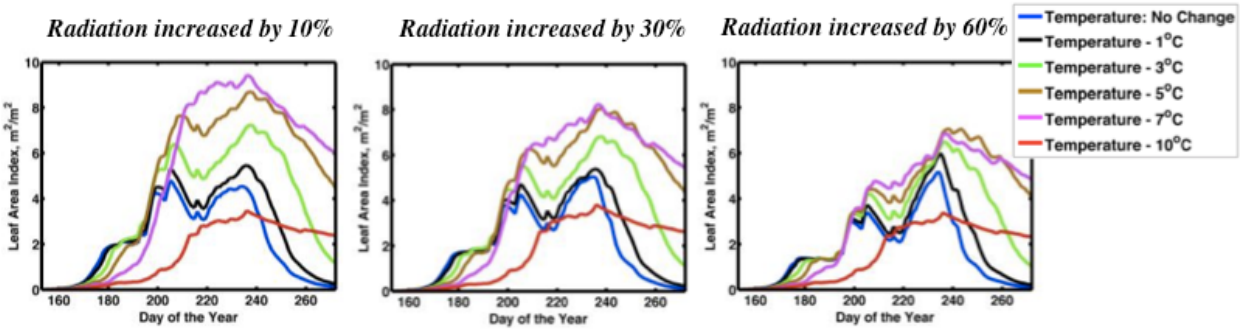

(a) *(b)* *(c)*

Figure 2.17 Leaf Area Index with (a) radiation increased by 10%, (b) radiation increased by 30%, (c) radiation increased by 60%. In each case, temperature was increased by 1, 3, 5, 7 & 10°C.

2.3.2b *Precipitation and temperature*

In this section, the combined effect of changing precipitation and temperature on crop

growth is presented.

(i) Decreased Precipitation and Decreased Temperature

Decreasing precipitation and decreasing temperature both change available soil moisture but in opposite directions. When precipitation was decreased available moisture reduced but when temperature was decreased, soil evaporation reduced and more moisture was available to plants leading to an increased growth. After sufficient moisture was available any further decrease in temperature reduced growth. In Figure 2.18a & b, growth increased until temperature was decreased to 7ºC but any further decrease in temperature decreased growth. When precipitation was reduced by 100% (precipitation = 0) (Figure 2.18c), growth did not increase until temperature was reduced by 10ºC.

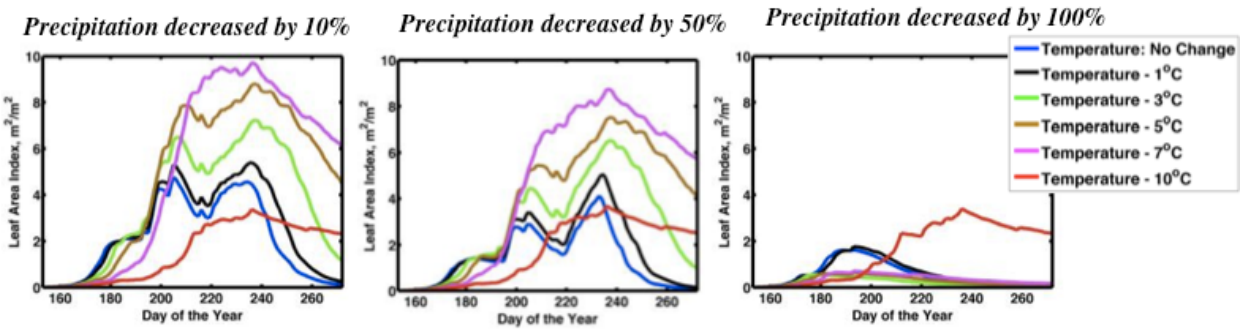

(a) *(b)* *(c)*

Figure 2.18 Leaf Area Index with (a) precipitation decreased by 10%, (b) precipitation decreased by 50%, (c) precipitation decreased by 100%. In each case, temperature was decreased by 1, 3, 5, 7 & 10ºC.

(ii) Increased Precipitation and Increased Temperature

Increasing both temperature and precipitation led to an overall decrease in growth (Figure 2.19) but for a particular temperature growth slightly increased with increased precipitation.

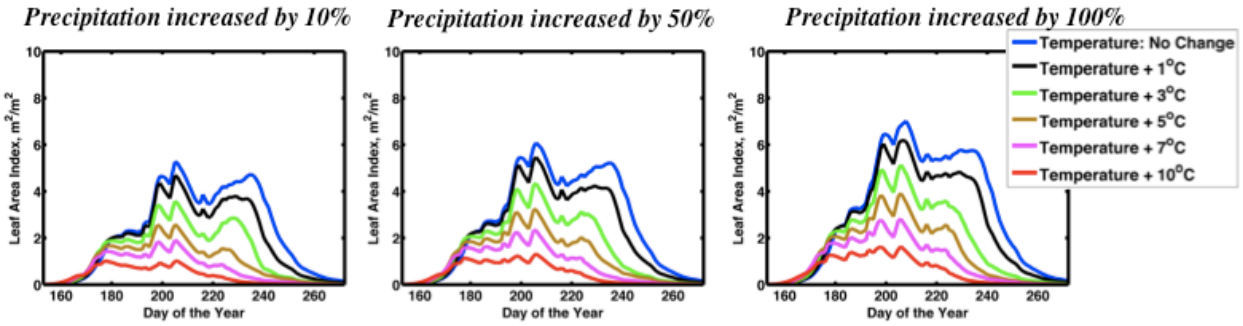

(a) *(b)* *(c)*

Figure 2.19 Leaf Area Index with (a) precipitation increased by 10%, (b) precipitation increased by 50%, (c) precipitation increased by 100%. In each case, temperature was increased by 1, 3, 5, 7 & 10°C.

(iii) Increased Precipitation and Decreased Temperature

Increasing precipitation and decreasing temperature increased growth upto a certain threshold temperature but any decrease in temperature beyond that reduced growth. This threshold temperature increased with increased precipitation. At 10% decrease in temperature (Figure 2.20a), growth increased until 7°C decrease in temperature and reduced thereafter. However, when precipitation was increased by 50% (Figure 2.20b) and 100% (Figure 2.20c), the growth increased until a decrease of 5°C in temperature and reduced thereafter. At a particular temperature, an increased precipitation increased growth.

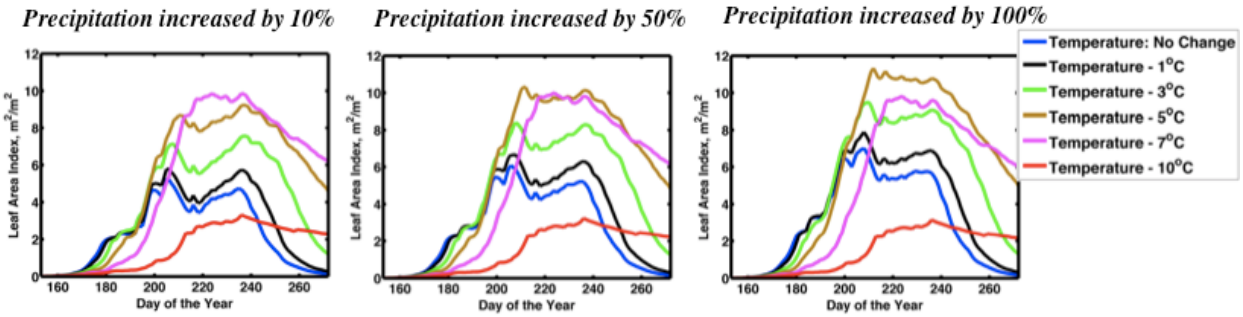

(a) *(b)* *(c)*

Figure 2.20 Leaf Area Index with (a) precipitation increased by 10%, (b) precipitation increased by 50%, (c) precipitation increased by 100%. In each case, temperature was decreased by 1, 3, 5, 7 & 10°C.

(iv) Decreased Precipitation and Increased Temperature

Decreasing precipitation and increasing temperature both increased soil water evaporation resulting in reduced moisture availability. Limited supply of moisture led to an inhibited growth (Figure 2.21).

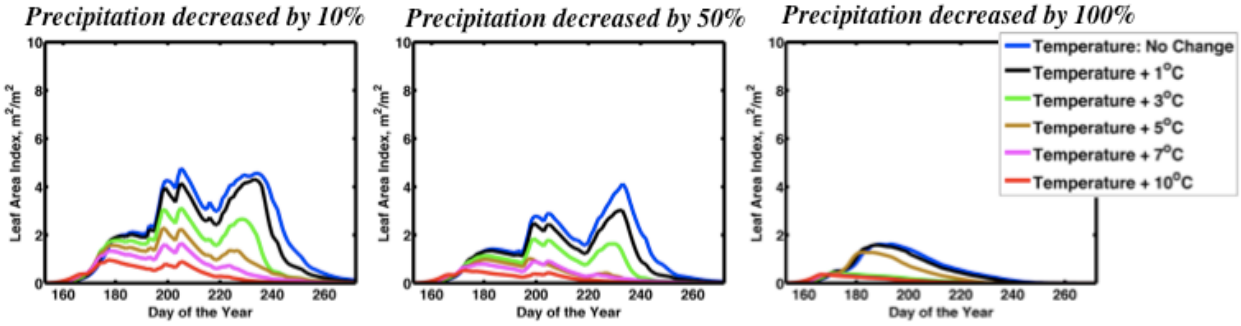

(a) *(b)* *(c)*

Figure 2.21 Leaf Area Index with (a) precipitation decreased by 10 %, (b) precipitation decreased by 50 %, (c) precipitation decreased by 100 %. In each case, temperature was increased by 1, 3, 5, 7 & 10°C.

2.3.2c *Incoming shortwave and precipitation*

Incoming short wave radiation provides PAR and controls soil moisture content by evaporation and precipitation is an important source of moisture. In this section, these two variables were changed simultaneously. The net affect on the growth was found to be a non-linear combination of the two and in most of the cases was controlled by moisture availability.

(i) Decreased Radiation and Decreased Precipitation:

Decreasing incoming shortwave radiations increased moisture availability by reducing evaporation and reduced photosynthetically active radiation. Reducing precipitation reduced soil moisture content. For small decrease in precipitation, this decrease in moisture content was compensated by reduced evaporation. For instance, in Figure 2.22 a & b, growth for 10% and 20% decrease in precipitation is quite similar to the case with no change in precipitation but any

decrease in precipitation beyond that reduced growth. At 60% decrease in radiation (Figure 2.22c), insufficient supply of PAR further contributed in reducing growth.

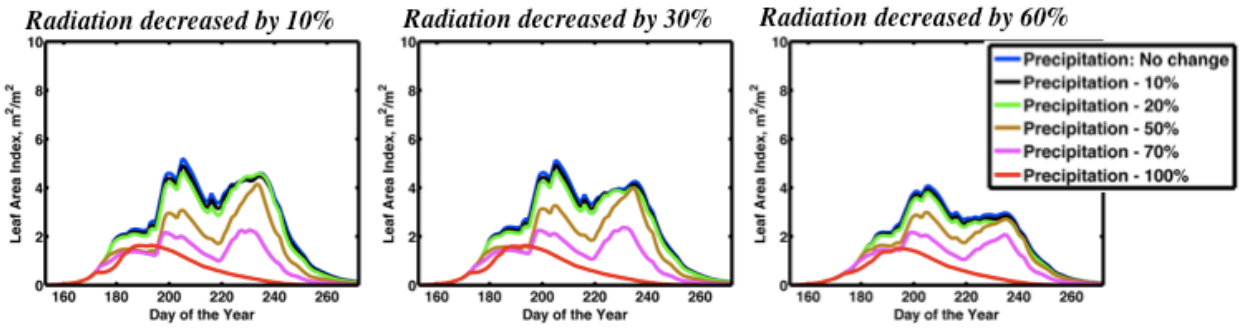

(a) (b) (c)

Figure 2.22 Leaf Area Index with (a) radiation decreased by 10%, (b) radiation decreased by 30%, (c) radiation decreased by 60%. In each case, precipitation was decreased by 10, 20, 50, 70 & 100%.

(ii) Increased Radiation and Increased Precipitation:

Increasing radiation reduced moisture availability and increasing precipitation increased it. Increased radiation also provided abundant supply of PAR. Increasing both radiation and precipitation, first increased growth as compared to the no change in precipitation case by a small amount but with a higher increase in precipitation accelerated the increase in growth (Figure 2.23).

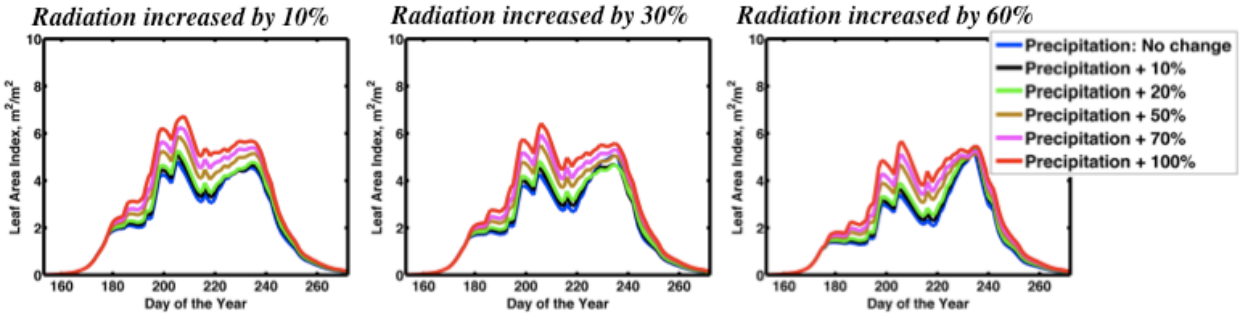

(a) (b) (c)

Figure 2.23 Leaf Area Index with (a) radiation increased by 10%, (b) radiation increased by 30%, (c) radiation increased by 60%. In each case, precipitation was increased by 10, 20, 50, 70 & 100%.

(iii) Increased Radiation and Decreased Precipitation:

Increasing radiation and decreasing precipitation led to reduced soil moisture content. The growth reduced due to a limited supply of soil moisture (Figure 2.24).

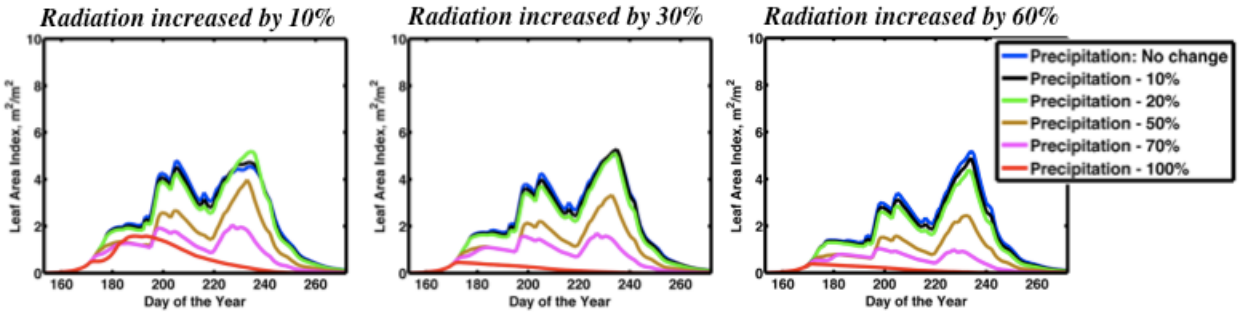

(a) *(b)* *(c)*

Figure 2.24 Leaf Area Index with (a) radiation increased by 10%, (b) radiation increased by 30%, (c) radiation increased by 60%. In each case, precipitation was decreased by 10, 20, 50, 70 & 100%.

(i) Decreased Radiation and Increased Precipitation:

Increasing precipitation and decreasing radiation both increased soil moisture content. Initially, the growth increased (Figure 2.25a &b), but a large decrease in radiation of around 60% reduced growth (Figure 2.25c).

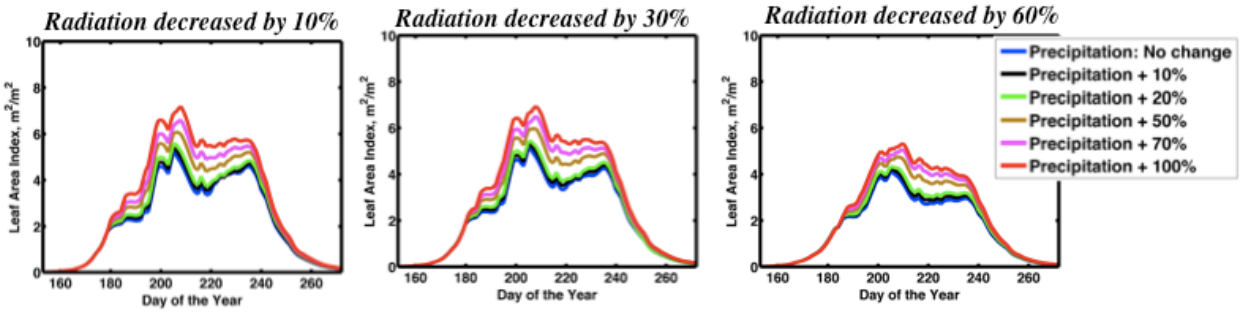

(a) *(b)* *(c)*

Figure 2.24 Leaf Area Index with (a) radiation decreased by 10%, (b) radiation decreased by 30%, (c) radiation decreased by 60%. In each case, precipitation was increased by 10, 20, 50, 70 & 100%.

2.4 Conclusion

- The crop growth model based on the SUCROS model was able to successfully simulate crop growth over the ameriflux soybean site in Nebraska.

- Sensitivity studies were conducted to understand the atmosphere-cropland response over the site.
- Decreasing temperature reduced growth in the juvenile stage and increased growth in the remaining season. However, a minimum temperature threshold of 7ºC was observed and any decrease in temperature beyond 7ºC decreased growth. Increasing temperature increased growth in juvenile stage and reduced growth in the mature stage. Life span of plants was observed to vary inversely with temperature.
- Growth was observed to vary directly with precipitation. The soil moisture cut off was found to be at 60% saturation. Any increase in soil moisture above this value reduced growth. Growth was also observed to increase with increasing initial soil moisture content.
- Decreasing incoming shortwave radiation increased growth but any decrease in radiation above 30% reduced the growth. Increasing radiation over the entire season reduced growth due to reduced moisture availability. The days when incoming radiation was low, increase in radiation was observed to increase the growth.
- Changing two variables at a time helped in understanding the combined effect of the variables. The variables either act synergistically or competitively in influencing growth.

List of Symbols

a_{srq} : Assimilate (CH_2O) requirement for dry matter production, g CH_2O g^{-1} DM

a_{dvs} : Factor accounting for effect of development stage on a_p

a_{lv} : Assimilate requirement for leaf dry matter production, g CH_2O g^{-1} DM leaf

$a_{\max}$: Actual CO2 assimilation rate at light saturation for individual leaves, g CO_2 m^{-2} leaf s^{-1}

a_p : Potential CO2 assimilation rate at light saturation for individual leaves, g CO2 m^{-2} leaf s^{-1}

a_{rt} : Assimilate requirement for root dry matter production, g CH_2O g^{-1} DM leaf

a_{st} : Assimilate requirement for stem dry matter production, g CH_2O g^{-1} DM leaf

a_{so} : Assimilate requirement for storage organ dry matter production, g CH_2O g^{-1} DM leaf

a_{tmp} : Factor accounting for effect of daytime temperature on a_p

c : Conversion factor for remobilization of stem carbohydrates into glucose

C : Daily total gross CH_2O assimilation of the crop, g CH_2O m^{-2} ground d^{-1}

c_f : Cluster factor

d : Day of the year, d

dt_{eff} : Daily effective temperature, °C

D_a : Daily total gross CO_2 assimilation of the crop, g CO_2 m^{-2} ground d^{-1}

d_{em} : Day of emergence, d

D_l : Death rate of leaf area, m^2 m^{-2} d^{-1}

d_l : Daylength, h d^{-1}

d_r : Development rate, d^{-1}

d_{rp} : Drying power term in Penman equation, mm d^{-1} kPa $°C^{-1}$

D_r : Relative death rate of leaves, d^{-1}

D_{rdv} : Relative death rate due to developmental ageing, d^{-1}

D_{rss} : Relative death rate due to self-shading at high LAI, d^{-1}

d_s : Development stage of the crop

d_t : Time interval of integration, d

D_t: Total gross CO2 assimilation of the crop, g CO_2 m^{-2} ground s^{-1}

e: Parameter to indicate emergence

e_d: Potential soil evaporation due to drying power of the air, mm/d

e_{rad}: Potential soil evaporation due to radiation, mm/d

e_{ff}: Initial light conversion factor for individual leaves, g CO_2 / J

e_{rt}: Rate of root elongation, mm/d

e_{rtc}: Constant for root elongation, mm/d

f_{cst}: Mass fraction carbon in the stems, g C g^{-1} DM

f_{gl}: CO2 assimilation rate at one depth in the canopy, g CO_2 m^{-2} leaf s^{-1}

f_{grs}: Intermediate variable for calculation of assimilation of sunlit leaves

f_{grsh}: CO2 assimilation rate at one depth in the canopy for shaded leaves, g CO2 m^{-2} leaf s^{-1}

f_{gros} : Instantaneous canopy CO2 assimilation, g CO2 m^{-2} ground s^{-1}

f_{grsun}: CO2 assimilation rate at one depth in the canopy for sunlit leaves, g CO2 m^{-2} leaf s^{-1}

f_{lv}: Fraction of shoot dry matter allocated to leaves

f_{rt}: Fraction total dry matter allocated to roots

f_{rtrl}: Fraction stem weight eventually translocated to storage organs

f_{sh}: Fraction total dry matter allocated to shoots

f_{sll}: Fraction of sunlit leaf area

f_{st}: Fraction of shoot dry matter allocated to stems

f_{so}: Fraction of shoot dry matter allocated to storage organs

G : Net growth rate of leaf area index, m^2 leaf m^{-2} ground d^{-1}

G_{lv} : Dry matter growth rate of leaves, g DM m^{-2} ground d^{-1}

G_r : Gross growth rate of crop dry matter, including translocation, g DM m^{-2} ground d^{-1}

G_{rt} : Dry matter growth rate of roots, g DM m^{-2} ground d^{-1}

G_{st} : Dry matter growth rate of stems, g DM m^{-2} ground d^{-1}

G_{so} : Dry matter growth rate of storage organs, g DM m^{-2} ground d^{-1}

I : Actual amount of precipitation intercepted by the canopy, mm/d

i : Interception capacity of precipitation of 1 layer of leaves, mm/d

K_{bl} : Extinction coefficient for direct component of direct PAR flux, m^2 ground m^{-2} leaf

K_{df} : Extinction coefficient for leaves, m^2 ground ha^{-1} leaf

K_{drt} : Extinction coefficient for total direct PAR flux, m^2 ground ha^{-1} leaf

L : Leaf area index, m^2 leaf m^{-2} ground

L_c : Leaf area index above selected height in canopy, m^2 leaf m^{-2} ground

l : Latent heat of evaporation of water J $Kg^{-1}H_2O$

M : Maintenance respiration rate of the crop, g CH_2O m^{-2} d^{-1}

M_{dvs} : Factor accounting for effect of DVS on maintenance respiration

M_{lv} : Maintenance respiration coefficient of leaves, g CH_2O g^{-1} DM d^{-1}

M_r : Maintenance respiration rate of the crop at reference temperature, g CH_2O m^{-2} d^{-1}

M_{rt} : Maintenance respiration coefficient of roots, g CH_2O g^{-1} DM d^{-1}

M_{st} : Maintenance respiration coefficient of stems, g CH_2O g^{-1} DM d^{-1}

M_{so} : Maintenance respiration coefficient of roots, g CH_2O g^{-1} DM d^{-1}

M_t : Factor accounting for effect of temperature on maintenance respiration

n_{rad} : Net radiation, J m^{-2} d^{-1}

P : Factor that accounts for reduced photosynthesis due to water stress

P_{df} : Instantaneous diffuse flux of incoming PAR, J m^{-2} ground s^{-1}

P_{dr} : Instantaneous direct flux of incoming PAR, J m^{-2} ground s^{-1}

p : Psychromatic instrument constant, kPa °C^{-1}

p_e : Potential soil evaporation, mm d^{-1}

p_t : Potential transpiration rate derived from Penman evaporation mm d^{-1}

p_{et} : Potential evapotranspiration, mm d^{-1}

r : Relative growth rate of leaf area during exponential growth, (°C $d)^{-1}$

R_{fh}: Reflection coefficient for diffuse PAR

R_{fs} : Reflection coefficient for direct PAR

R : Daily Precipitation, mm/d

R_{off} : Runoff, mm/d

S : Tangent of the relationship between saturated vapor pressure and temperature, kPa °C^{-1}

s : Scattering coefficient of leaves for PAR

s_a : Specific leaf area, m^2 leaf g^{-1} leaf

s_b : Sine of solar elevation

t_{eff} : Factor accounting for effect of temperature on maintenance respiration

t : Time interval of integration, d

T : Translocation rate of stem dry matter to storage organs, g DM m^{-2} d^{-1}

T_{l1}: Thickness of first soil layer, mm

T_{l2} : Thickness of second soil layer, mm

T_{l3}: Thickness of third soil layer, mm

T_{l4} : Thickness of forth soil layer, mm

V_{pp}: Absorbed light flux by leaves perpendicular on direct beam, J m^{-2} leaf s^{-1}

V_{sd}: Absorbed direct component of direct flux per unit leaf area (at depth L_c), J m^{-2} leaf s^{-1}

V_{sdf}: Absorbed diffuse flux per unit leaf area (at depth L_c), J m^{-2} leaf s^{-1}

V_{sshd}: Total absorbed flux for shaded leaves per unit leaf area (at depth L_c), J m^{-2} leaf s^{-1}

V_{st}: Absorbed total direct flux per unit leaf area (at depth L_c), J m^{-2} leaf s^{-1}

V_{sun}: Total absorbed flux for sunlit leaves in one of three Gauss point classes, J m^{-2} leaf s

W_{lv}: Dry weight of the leaves (green + dead), g m^{-2}

W_{rt}: Dry weight of the roots, g m^{-2}

W_{so}: Dry weight of storage organs, g m^{-2}

W_{st}: Dry weight of the stem, g m^{-2}

W_{gauss}: Array containing weights to be assigned to Gauss points

w_{st1}: Water content at soil saturation for layer 1, cm^3 water/cm^3 soil

w_{l1}: Amount of water in the first soil compartment, mm

w_{sert}: Auxiliary variable to calculate root extension

X_{gauss}: Array containing Gauss points

z_{rt}: Rooted Depth, mm

CHAPTER 3

COUPLED MODEL: DEVELOPMENT AND SENSITIVITY STUDY

The crop growth model described in the previous chapter simulates the forcing-response relationship between the atmospheric variables and the crop growth. In the model, the crop growth module is forced with the atmospheric data and variations in growth with changes in atmospheric variables are simulated. However, it does not have the capability to simulate the feedback from the crop growth back to the atmosphere. Moreover, the crop growth model is not spatially explicit, which restricts the model to simulate the crop growth only at a point or a plot scale. To study the feedbacks between atmosphere and croplands at a regional scale, a computationally efficient tool was developed. A crop growth module derived from the crop growth model SUCROS (Goudriaan & Van Laar 1994) was incorporated in the Weather Research Forecasting (WRF) model version 3 (Skamarock et al., 2008). This model has the capability to simulate dynamic crop growth. It simulates the response of crops with changing atmospheric variables and also feeds back the effect of crop growth on the atmosphere. This chapter focuses on the coupled model development and its ability to simulate the crop growth. In the first section of this chapter, the coupling procedure employed to incorporate the crop growth module in the WRF model is described and in the second section, experimental set up and a sensitivity study are presented.

3.1 Coupled Model Development

WRF is a non-hydrostatic mesoscale model. A detailed description of WRF version 3 can be found in Skamarock et al. (2008). In this section, the segments of WRF specific to the coupling are briefly described. WRF has a three-level physics structure consisting of solver, driver and individual schemes. The solver routine in the WRF model is responsible for calling

various physics and dynamics modules and it acts as a bridge to connect the two. The solver also controls parallel processing in the model. The physics drivers, which are called in the solver routine, call individual physics schemes by making a choice from different available schemes. These physics drivers act as a interface between the solver and the individual schemes.

The physics driver relevant to the coupling procedure is the surface physics driver. The surface physics module calls the land surface model. In this case the NOAH land surface model was called. The NOAH land surface model is made to call the crop growth module at a daily time step. The growth model receives the forcing data i.e., incoming shortwave, temperature, precipitation, evapotranspiration and soil moisture from the WRF model. It then calls different subroutines to simulate various growth processes. The crop growth module feeds back the computed LAI and root depth to the NOAH module at the end of each day (Figure 3.1).

Most parts of the WRF model are written in FORTRAN 90. For compatibility and consistency purposes, the crop growth was written in FORTRAN 90. WRF model does not allow the use of common blocks, so all the variables used in the growth model subroutines were passed through argument lists. First, the new variables were added to the registry files: Registry.EM & Registry.wrfvar to add the variables to the WRF model and make them available at different locations throughout the WRF code. A sample registry entry to add a new variable looked like the following:

state real x ij misc 1 - rhdu=(copy_fcnm) "x" "x description " "x-unit"

In the above example, the variable **x** is a two-dimensional variable with one time level. The strings **r** and **h** specify that the variable is subject to restart, history I/O classification and **u** and **d** accounts for the interpolation between the parent domain and the nest.

The variables were then initialized in the subroutine phy_init (in the module phys/module_phy_init.F) which is called in the module start_em.F in dyn_em directory. The variables were then passed to the surface physics driver (module_surface_driver.F in phys directory) and then through the NOAH driver module (module_sf_noahdrv.F in phys directory) to NOAH land surface model (SFLX subroutine in module_sf_noahlsm.F). The SFLX subroutine calls the SUCROS subroutine by passing the environmental parameters and the new variables. The plant growth in WRF model is represented by leaf area index (LAI). The

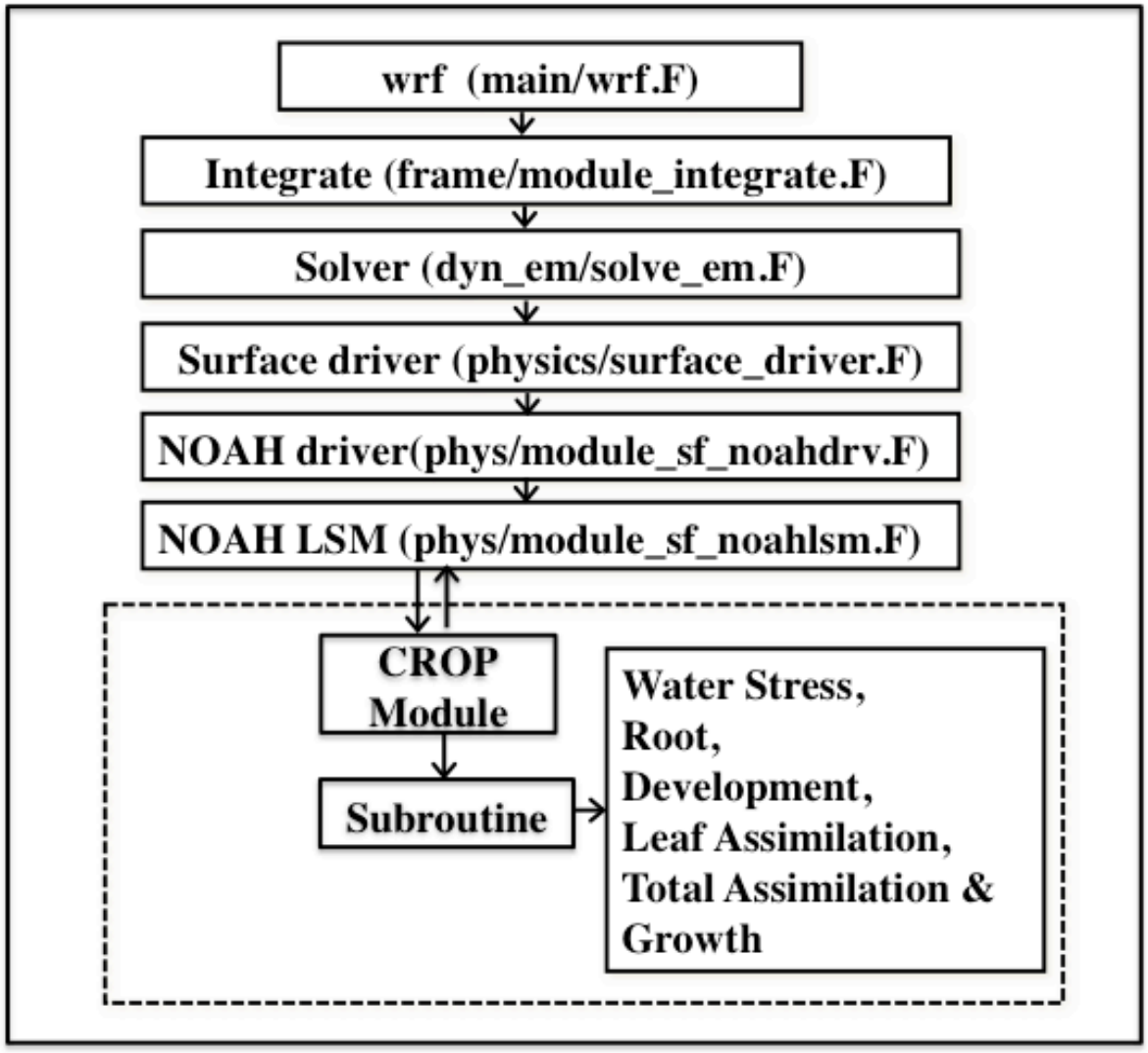

Figure 3.1 WRF code structure

SUCROS subroutine calculates average temperature, evapotranspiration and net radiation for a particular day. Soil moisture value is also provided to the growth model from NOAH land surface model. At the end of each day, vegetation processes described in sections 2.1.1 to 2.1.7 are simulated by calling the respective subroutines. The subroutines called are Water Stress, Root, Leaf Assimilation, Total Assimilation and Growth (Figure 3.1). The crop growth module feeds back Leaf Area Index and root depth to the NOAH land surface model. This accounts for the feedback from crops back to the atmosphere. A schematic diagram of the coupled WRF-SUCROS model is shown in Figure 3.2.

3.2 Coupled Model: Experimental Design & Sensitivity Study

A set of experiments was conducted to test the capability of the coupled WRF-CROP model in simulating the cropland-atmosphere feedbacks over different locations in the mid-western United States (Figure. 3.3). Two different soybean sites were selected (Table 3.1) from the Ameriflux website (http://public.ornl.gov/ameriflux/) located in Nebraska and Illinois. The experiments were conducted for one growing season for both the sites. The experiments lasted over approximately three months and were conducted at 2 km horizontal resolution using a nested domain (Figure 3.4) for both the sites. The effect of various atmospheric drivers such as moisture, temperature and radiation on the crop growth was analyzed by conducting simulations with modified parameterization.

A three nested domain was used in the experiments for both the sites. The size of the largest domain was 1600 km X 1600 km, the middle domain was 848 km X 848 km and the finest domain was 114 km X 114 km. Spatial horizontal grid resolutions of 32 km, 8 km and 2 km and time steps of 96 seconds, 24 seconds and 6 seconds were used for coarsest, middle and finest domains respectively. A vertical resolution of 28 eta levels was used for all three domains.

Domains for Nebraska site were centered at -96.43° East longitude, 41.17° North latitude and that for Bondville, IL site at -88.29° East longitude, latitude 40.00° North longitude. Landuse data was obtained from MODIS. In all the simulations, initial conditions were provided by GFS analysis obtained from http://nomads.ncdc.noaa.gov/data.php website. Lateral boundary conditions for the coarsest domain were also taken from GFS analysis. A summary of domain description is provided in Table 3.2.

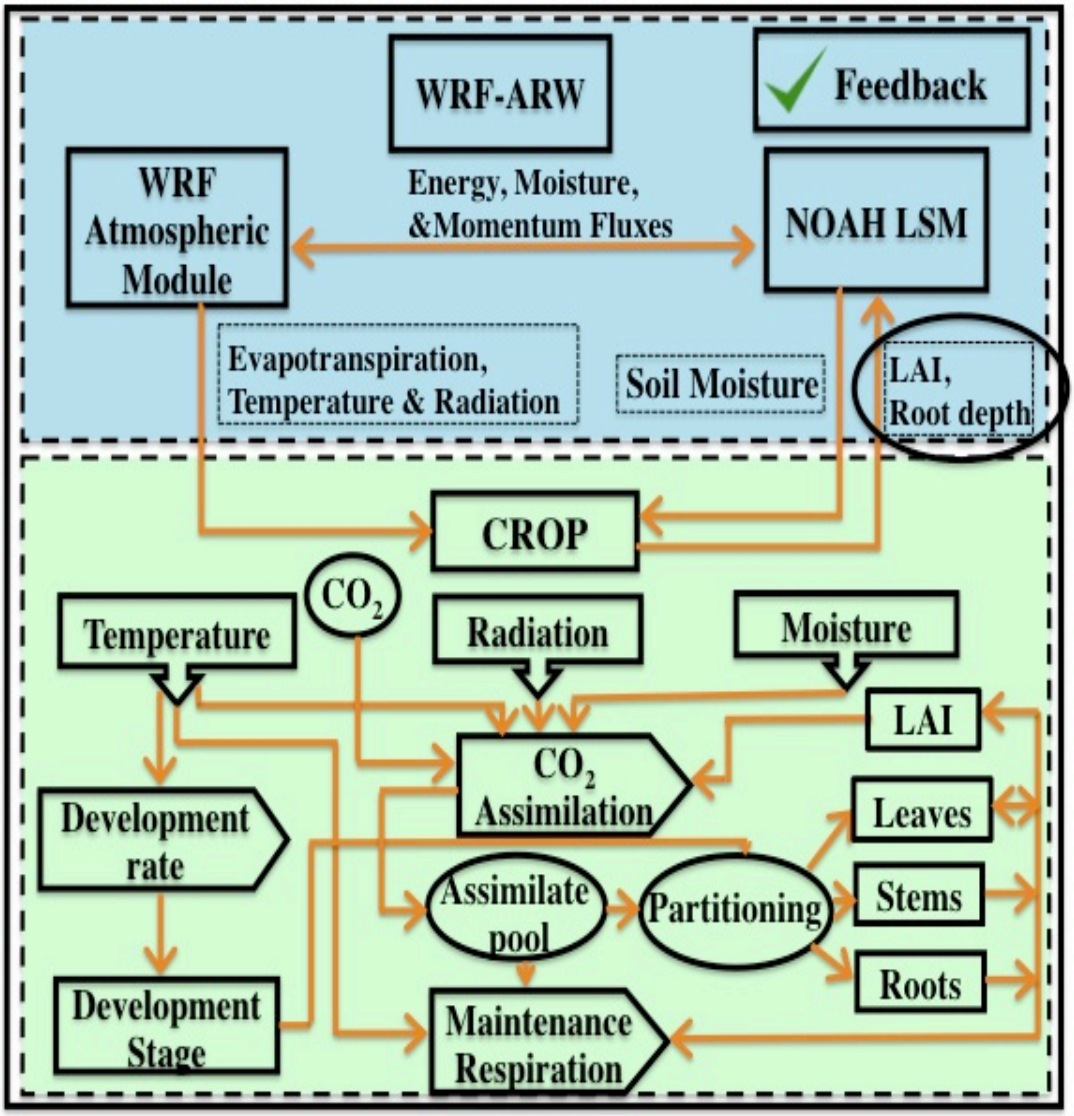

Figure 3.2 A schematic diagram of the coupled WRF-CROP model.

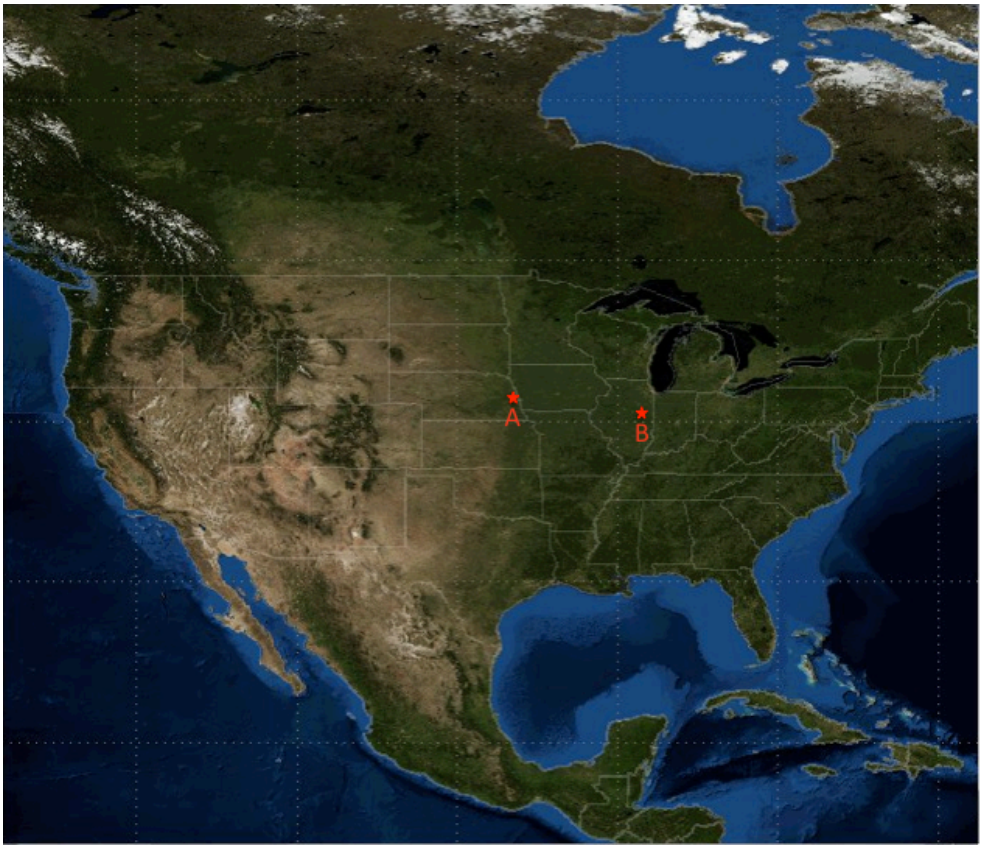

Figure 3.3 Location of the two sites, A: Nebraska, B: Bondville

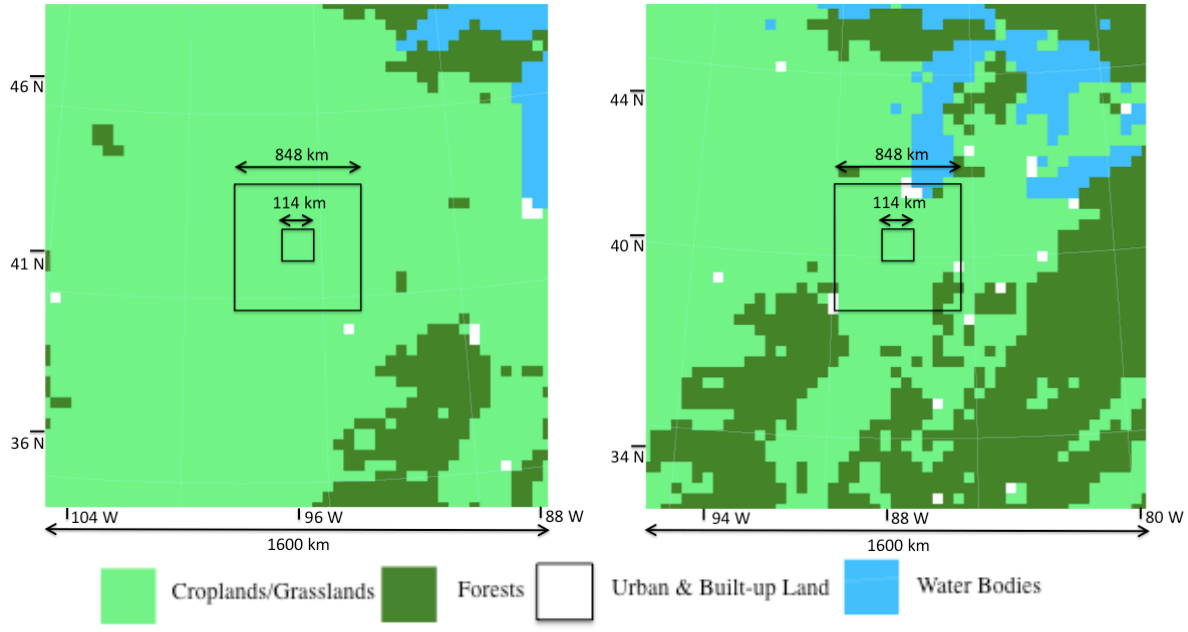

a) b)

Figure 3.4 Nested domain used in the simulations a) Nebraska site b) Bondville site

In all the simulations, I used Yonsei University scheme for boundary layer physics, Monin-Obukhov similarity surface-layer scheme and Noah Land-Surface scheme. Kain-Fritsch Cumulus scheme was used for the two coarser domain and turned off for the finest domain. Rapid Radiative Transfer Model (RRTM scheme) and Dudhia scheme were used for longwave radiation and short wave radiation respectively. WRF Single-Moment 3-class simple ice scheme microphysics scheme was used in the simulations with microphysics turned on. Runge-Kutta 3rd order time-step integration was used. Turbulence and mixing options evaluated 2nd order diffusion term on coordinate surfaces. Horizontal Smagorinsky first order closure was used and horizontal diffusion was diagnosed from horizontal deformation and vertical diffusion was done by PBL scheme (2D). There was no damping and moisture and scalar advection were kept positive definite. Five rows were specified for boundary value nudging. A list of the physics and dynamics used in the experiments is provided in Table 3.3 and Table 3.4.

As discussed in the chapter 2, plant growth depends upon various atmospheric drivers such as temperature, radiation and precipitation. We analyzed the impact of each of these atmospheric variables on plant growth in section 2.2 using the standalone crop growth model. In this section, the experiments conducted with WRF-CROP coupled model are described. The dynamic nature of WRF-CROP coupled model allowed it to simulate not only the response of crop growth with changes in the atmospheric variables but also the feedback from the cropland back to the atmosphere.

The first set of experiments was done by running the WRF-CROP model over the two sites in the Midwestern United States with full model parameterization. It was observed that the precipitation events controlled the atmospheric fluxes such as latent heat and sensible heat over the croplands. To understand the effect of individual variables on growth, I modified the model

parameterization either by changing the namelist.input file or by modifying the code.

The second set of experiment was conducted by turning off the microphysics and the cumulus scheme, which inhibited the formation of precipitation and clouds in the model. In the absence of precipitation the soil moisture was not replenished and in the absence of clouds the croplands received almost same radiation throughout except for the changes in radiation due to air particle and water vapor scattering. The results from these experiments can be used to understand the effect of soil moisture and temperature on the crop growth.

In the third set of experiments, the code was modified in such a way that now cloud formed in the model but the precipitation was still inhibited. In the presence of clouds, the croplands received varying radiation. The effect of radiation on the growth under soil water stress scenario can be understood by comparing the second and the third sets of experiments.

In the fourth set of experiments, the conditions were kept same as the second set of experiments but now constant soil moisture was applied throughout the growing season. Under these conditions, the growth was simulated without any soil water stress. The effect of soil moisture on growth was studied by comparing second and forth sets of experiments. This experiment also helped in understanding the effect of crop growth on atmospheric drivers.

In the final set of experiments, the parameterization was same as the third set but constant soil moisture was supplied throughout the growing season. The effect of radiation on growth under constant soil moisture conditions was examined by comparing forth and final sets of experiments. A list of all the experiments is provided in Table 3.5.

3.2.1 Experiment 1: WRF-SUCROS Control Scenario

In the WRF-SUCROS control scenario, the coupled model was run over the two crop sites in the mid-western US with full parameterization. The coupled model was able to simulate

crop growth over the entire growth season for both the sites (Figure 3.5). The growth at the Bondville site was observed to be higher than the Nebraska site. This can be attributed to a lower

Site	Latitude/Longitude of the center	Season Simulated	Crop Type
US-Ne3, Nebraska	**41.17, -96.43**	**2006**	**Soybean**
US-Bo1, Bondville, Illinois	**40.00, -88.29**	**2006**	**Soybean**

Table 3.1 Site Details

Domain	
Horizontal	
Domain1	**Size: 1600 km X 1600 km Resolution: 32 km**
Domain2	**Size: 848 km X 848 km Resolution: 8 km**
Domain3	**Size: 114 km X 114 km Resolution: 2 km**
Vertical	**28 Eta-Levels**
Time Step	**Domain1: 96 seconds Domain2: 24 seconds Domain3: 6 seconds**
Landuse	**MODIS data**
Initial Condition	**GFS Analysis**

Table 3.2 Details of Domain Configuration.

Physics	
Cumulus scheme	**Kain-Fritsch scheme**
PBL Physics	**Yonsei University scheme**
Longwave Physics	**Rapid Radiative Transfer Model scheme**
Shortwave Physics	**Dudhia scheme**
Land Surface Physics	**NOAH LSM**
Surface Layer Physics	**Monin-Obukhov similarity scheme**

Table 3.3 Details of Physics used in the model

Dynamics	
Time Integration	**Runge-Kutta 3rd order**
Horizontal Diffusion	**Smagorinsky first order closure**
Vertical Diffusion	**From PBL scheme**

Table 3.4 Details of Dynamics used in the model

Experiments	**Parameterization**	
Experiment 1. WRF-CROP/ Control Scenario	**Microphysics on, Cumulus scheme on**	**Rain: YES Clouds: YES Soil moisture: Dynamic**
Experiment 2.	**No microphysics, No cumulus scheme**	**Rain: NO Clouds: NO Soil moisture: Dynamic**
Experiment 3.	**Modified Microphysics, No cumulus scheme**	**Rain: NO Clouds: YES Soil moisture: Dynamic**
Experiment 4.	**No microphysics, No cumulus scheme**	**Rain: NO Clouds: NO Soil moisture: Constant**
Experiment 5.	**Modified Microphysics, No cumulus scheme**	**Rain: NO Clouds: YES Soil moisture: Constant**

Table 3.5 List of experiments for each site.

temperature at the Bondville site as compared to the Nebraska site especially in the first half of the growing season. Lower temperature reduced soil water evaporation increasing soil water availability to plants (Figure 3.6) and also reduced maintenance respiration of the plants resulting in a higher growth at the Bondville site while higher temperature at Nebraska site increased respiration requirements of the plants and also increased soil water evaporation reducing growth. The atmospheric fluxes in this experiment were controlled mainly by the rainfall events, which made it difficult to understand the effect of individual atmospheric drivers on the growth and the feedback of growth on the drivers. So, to analyze the feedback loop on individual atmospheric

variables several experiments with modified parameterization were conducted. These experiments are discussed below.

3.2.2 Experiment 2: Effect of Moisture

The aim of this experiment was to test the ability of the coupled model to simulate the effect of soil moisture on the crop growth. A scenario with no rain and no clouds was created by switching off microphysics and cumulus schemes in the model. In the absence of precipitation, soil moisture was not replenished and fell below wilting point after certain time, which resulted in reduced crop growth at both the crop sites (Figure 3.5). Initially, the plants grew using the initial soil moisture content but died quickly as soon as soil moisture became inadequate (Figure 3.6). Decrease in soil moisture with time due to the absence of precipitation also resulted in an increased sensible heating (Figure 3.7), and reduced latent heating (Figure 3.8). This in turn led to decreased water vapor (Figure. 3.9) and an increased temperature (Figure 3.10) and as compared to the WRF-CROP control scenario in experiment 1. Increased temperature further reduced soil moisture by increasing soil water evaporation. The maintenance respiration requirements of the plants also increased in increased temperature scenario. Thus, the combined affect of insufficient soil moisture and enhanced temperature reduced the overall growth.

3.2.3 Experiment 3: Effect of Radiation under dynamic soil moisture

The purpose of this experiment was to investigate the effect of radiation on the crop growth under water stress conditions. In this experiment, WRF Single-Moment 3-class microphysics scheme was turned on but the code was modified in such a way that clouds and water vapor formed but there was no precipitation and the cumulus scheme was turned off. Since there were no clouds in experiment 2, the radiation in the region was only effected by scattering from the air particles and water vapor. However, in this case, the presence of cloud produced

variable incoming radiation as compared to almost constant radiation in Experiment 2. The incoming shortwave radiation reduced due to the presence of clouds as compared to Experiment 2 (Figure 3.11). Since the moisture supply was still inadequate (Figure 3.6), the growth was low (Figure 3.5). However, the presence of cloud reduced radiation supply, which reduced evaporation and increased moisture availability as compared to Experiment 2. This increased growth by a small amount in the latter half of the growth cycle. Decrease in incoming radiations also reduced photosynthetically active radiations (PAR) but under water stress conditions the effect of reduced PAR was not significant. Reduced incoming shortwave radiation also resulted in reduced sensible heating (Figure 3.7) and temperature (Figure 3.10) as compared to experiment 2 while the changes in other variables such as latent heat (Figure 3.8) and water vapor (Figure 3.9) were small due to only a small change in LAI as compared to experiment 2.

3.2.4 Experiment 4: Effect of Temperature

In this case, we studied the effect of temperature by supplying constant soil moisture throughout the growing season. Microphysics and cumulus scheme were turned off while constant soil moisture (0.29 m^3/m^3) was supplied throughout the growing season. Under constant availability of moisture, plant growth and leaf area index increased as compared to experiment 1, 2 and 3 (Figure 3.5). Latent heat flux (Figure 3.8) also increased while Sensible heat (Figure 3.7) decreased in this case as compared to experiment 1, 2 and 3. Sensible heat flux and latent heat flux were directly regulated by the crop growth. Latent heat flux was observed to vary directly with the LAI while sensible heat varied inversely with LAI over the entire season. Water vapor in this case increased (Figure 3.9) and temperature decreased (Figure 3.10) as compared to experiment 2 and 3 while the change in these variables as compared to experiment 1 was inconsistent. Decreased temperature reduced respiratory requirements of the plants and enhanced

the growth. Reduced temperature and constant supply of moisture together increased growth. However, it was difficult to understand only the individual impact of temperature, as changes in growth and temperature were dependent on each other.

3.2.5 Experiment 5: Effect of Radiation under constant soil moisture

This experiment analyzed the effect of radiation under constant supply of soil moisture. In this case the microphysics scheme was turned on but the code was modified in such a way that water vapor and cloud formed but there was no precipitation in the model and cumulus scheme was still switched off. This resulted in a scenario with variable radiation and no precipitation over the region in the model but constant soil moisture was applied throughout the season. The presence of cloud resulted in a reduced incoming shortwave radiation over the domains (Figure 3.11), which in turn reduced net sensible (Figure 3.7) and latent heat flux (Figure 3.8) as compared to experiment 4. Temperature also decreased as compared to experiment 4. Reduced incoming radiation also led to a reduced supply of PAR while reduced temperature reduced maintenance requirements of the crop. These two factors affect the growth in opposite manner and the net impact on the growth is a non-linear combination of the two. The effect of reduced

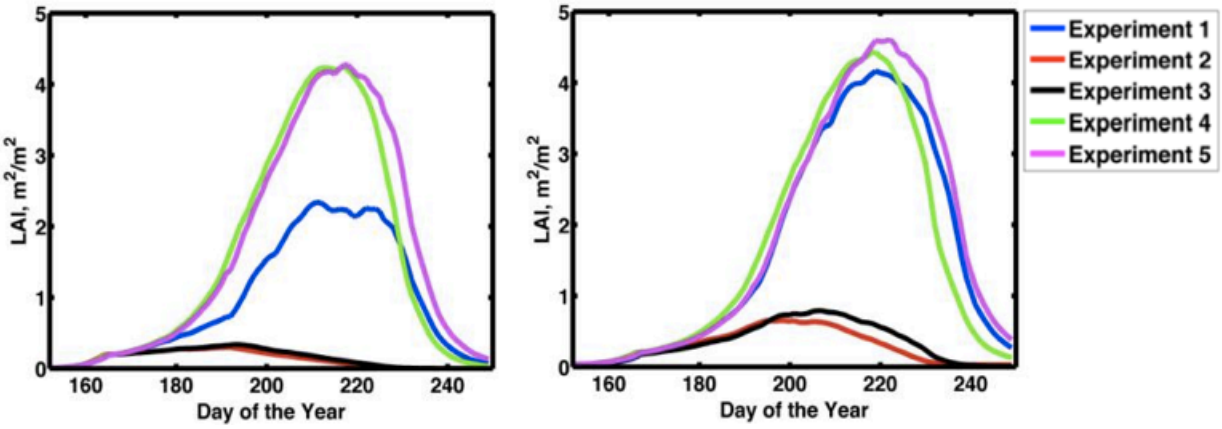

(a) *(b)*

Figure 3.5 Domain averaged Leaf area index at a) Nebraska site b) Bondville site

radiation dominated in the first half of the growing season when growth reduced and impact of reduced temperature dominated in the latter half where growth was observed to increase (Figure 3.5). However, due a small difference in radiation between the two experiments the change in LAI was also small.

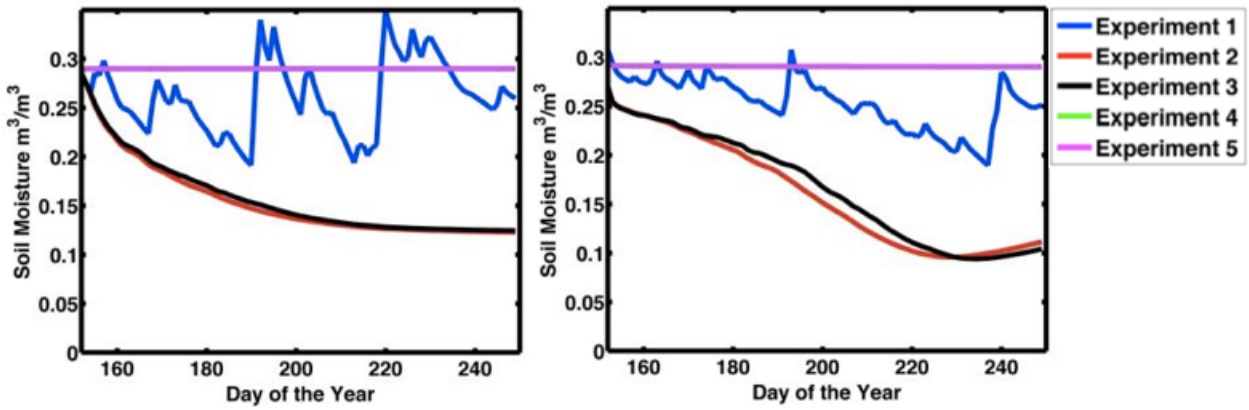

(a) *(b)*

Figure 3.6 Domain averaged volumetric soil moisture for layer 1 at a) Nebraska site b) Bondville site

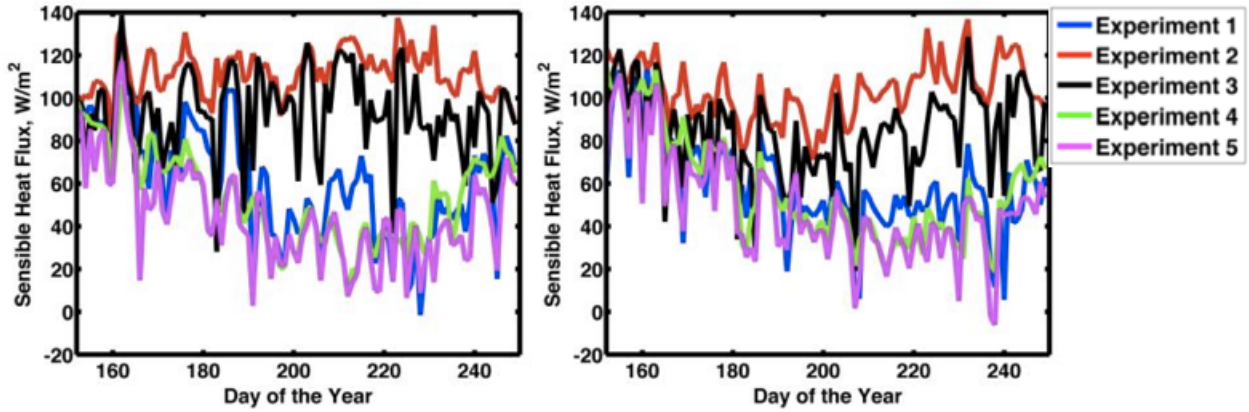

(a) *(b)*

Figure 3.7 Domain averaged Sensible heat flux at a) Nebraska site b) Bondville site

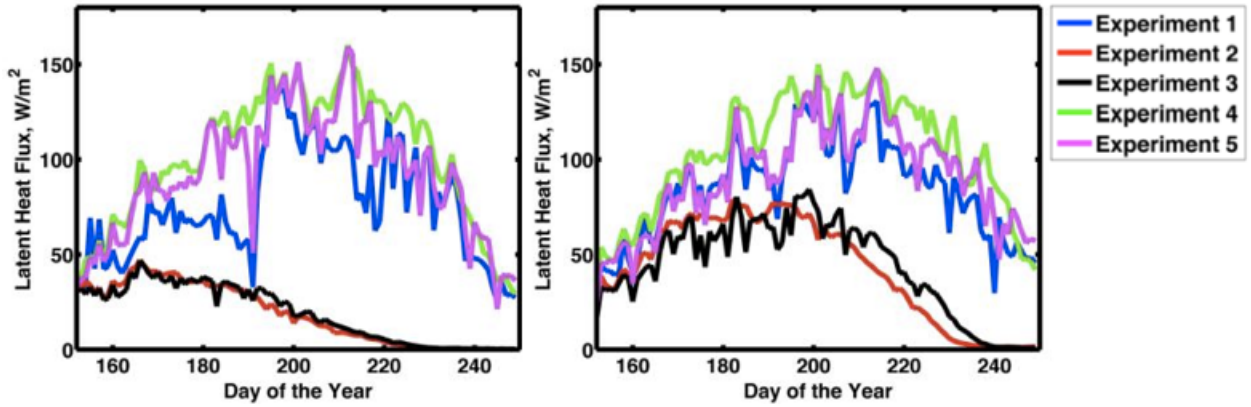

(a) *(b)*

Figure 3.8 Domain averaged Latent heat flux at a) Nebraska site b) Bondville site

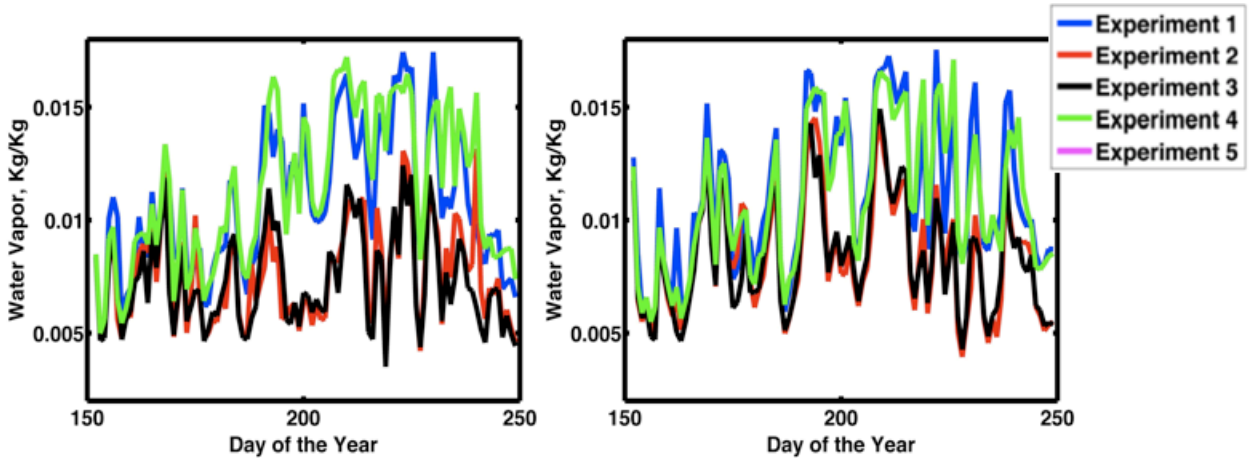

(a) *(b)*

Figure 3.9 Domain averaged water vapor for a) Nebraska site b) Bondville site

3.3 Conclusion

- The vegetation module of the crop growth model, SUCROS was successfully incorporated in the WRF model. The WRF-CROP coupled model was run to simulate the crop growth over the two soybean sites in Nebraska and Illinois for the growing season of the year 2006.
- The effect of individual atmospheric variables such as precipitation, incoming shortwave radiation and temperature on the crop growth was studied by modifying the model parameterization.

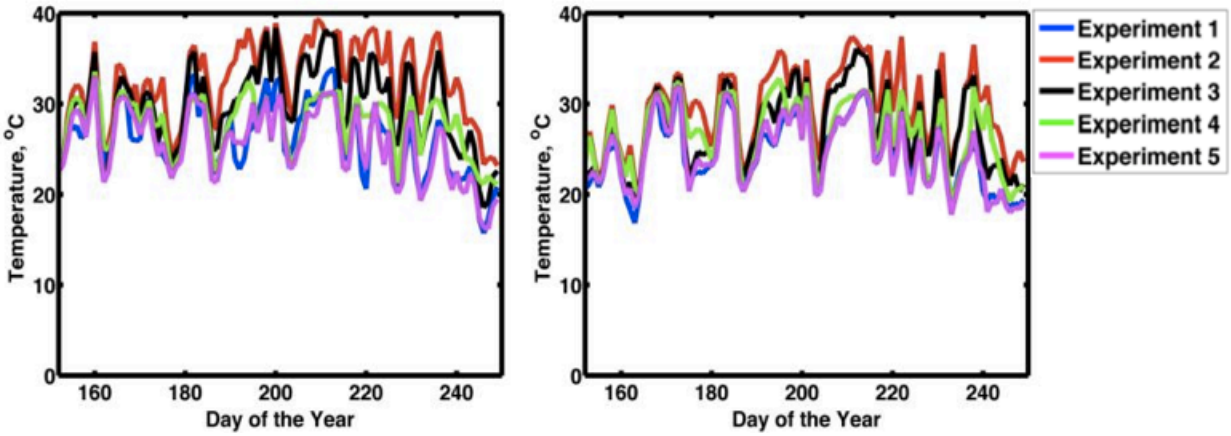

(a) *(b)*

Figure 3.10 Domain averaged Temperature at a) Nebraska site b) Bondville site

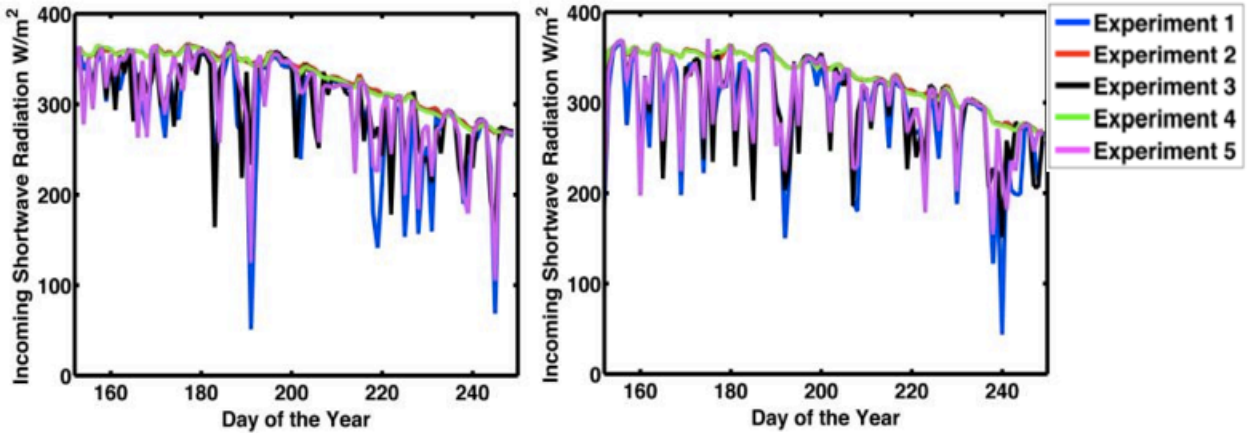

(a) *(b)*

Figure 3.11 Domain averaged Incoming shortwave radiation at a) Nebraska site b) Bondville site

- In the absence of precipitation, a soil water stress situation was created which reduced the crop growth while on supplying constant soil moisture under the no precipitation conditions the growth increased. Hence, the crop growth directly depends on the soil moisture.
- Incoming shortwave radiation plays an important role in the growth by controlling PAR and soil water evaporation. However, changes in incoming radiation also affected the air temperature. Changes in temperature affects growth by controlling soil water evaporation and respiration requirements of the plants. The net result on the growth was observed to be a non

linear combination of these two factors. The effect of radiation was studied by comparing the simulations with and without the clouds and difference in LAI for the two runs was found to be small.

- The growth was found to vary inversely with the air temperature. Warming was observed to reduce growth while cooling was observed to increase growth. At the same time changes in growth also directly affected temperature by changing the sensible heat flux.
- The sensitivity study was successfully able to test the performance of the coupled model in simulating growth with changing atmospheric drivers. The atmospheric fluxes i.e., sensible heat flux and latent heat flux over the croplands were also observed to vary directly with the growth. A large LAI value resulted in a large latent heat flux and a small sensible heat flux while a small LAI produced high sensible heat flux and low latent heat flux. Temperature and atmospheric moisture content were directly controlled by sensible heat flux and latent heat flux respectively. These change in the atmospheric variables with growing crops are the feedbacks of the crop growth on the atmosphere and are discussed in detail in the following chapter.

CHAPTER 4

COUPLED MODEL: EVALUATION & FEEDBACKS

In this chapter the WRF-CROP coupled model performance in terms of leaf area index simulation is evaluated and feedbacks from crops back to the atmosphere are analyzed by conducting a comparative study of results from WRF and WRF-CROP model experiments. WRF model assumes a constant crop cover over the croplands throughout the season while WRF-CROP coupled model simulates crop growth with changing atmospheric conditions and feeds back the calculated Leaf Area Index (LAI) and root depth to incorporate the effect of vegetation growth on the atmosphere.

4.1 Coupled Model Evaluation

Figure 4.1 shows the simulated LAI by WRF model and WRF-CROP coupled model and the LAI obtained from the observed data. The LAI MODIS observation data was available for both the sites and was obtained from https://lpdaac.usgs.gov/ website. The LAI station data was only available for the Nebraska site was obtained from the Ameriflux website http://public.ornl.gov/ameriflux/. WRF model has a constant LAI over the entire season while WRF-CROP model simulates dynamic crop growth. LAI simulated by the coupled model is comparable to the observed MODIS LAI data for both the sites. The simulated LAI for the Nebraska site is underestimated as compared to the Ameriflux station data.

4.2 Cropland-Atmosphere Feedbacks

As described in the previous chapter the WRF-CROP coupled model was developed by dynamically coupling a crop growth module to the WRF model. The dynamic coupling makes the model capable of simulating not only the crop growth with changing atmosphere but also the feedback from crop back to the atmosphere. The effect of atmosphere on the crop growth has

been discussed in the previous chapter. In this section, the effect of the crop growth on the atmospheric variables is investigated. A comparative study of results from the WRF-CROP

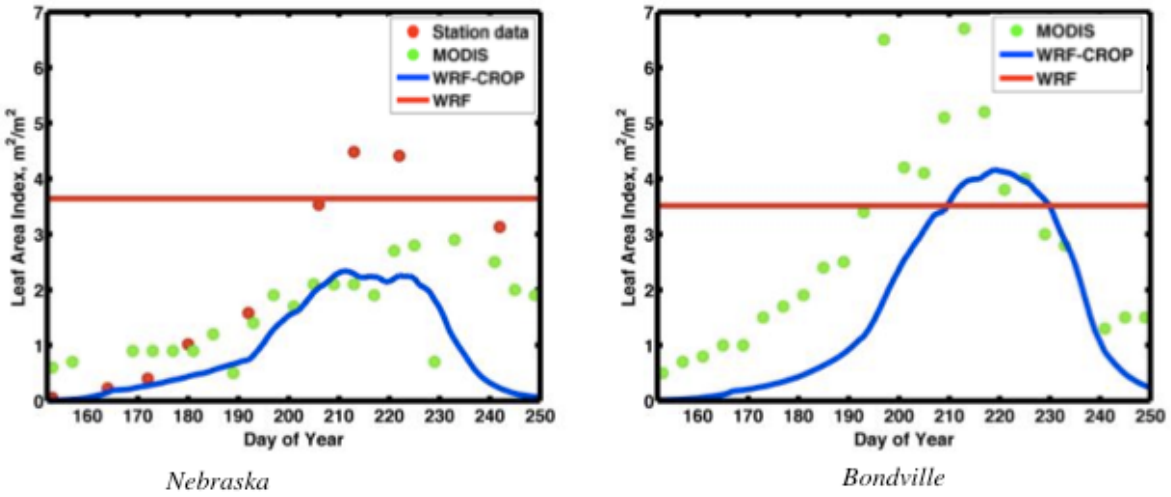

Figure. 4.1 Observed and Simulated Leaf area index at a) Nebraska site b) Bondville site.

coupled model and WRF model simulations explains the effect of dynamic growth on the atmosphere.

The two models, the WRF model and the WRF-CROP coupled model were run over the two locations in Nebraska and Illinois described in the previous chapter (Table 3.1). The same domain described in the previous was used in all the experiments (Table 3.2). Details about the sites and the domain are provided in chapter 3, section 3.2.

4.2.1 Experiment I

The first set of experiments was conducted with the full model parameterization provided in table 3.3 and table 3.4. The growth in WRF model was constant and leaf area index was around 3.5 m^2/m^2 throughout the growing season for both the sites. On the other hand, the growth in the WRF-CROP model was dynamically varying with the atmosphere. LAI increased to a maximum value of around 4 m^2/m^2 for the Bondville site and to approximately 2.5 m^2/m^2 for the Nebraska site (Figure 4.2) and as the plant aged LAI start to decrease due to shelf shading

and ageing of the leaves. In the first half of the growing season, LAI for WRF-CROP model simulations is smaller than WRF model simulation for both the sites which results in a smaller latent heat flux for WRF-CROP runs as compared to the WRF runs over both the sites (Figure 4.3). However, as the difference in LAI for the two model runs decreased, the difference in latent

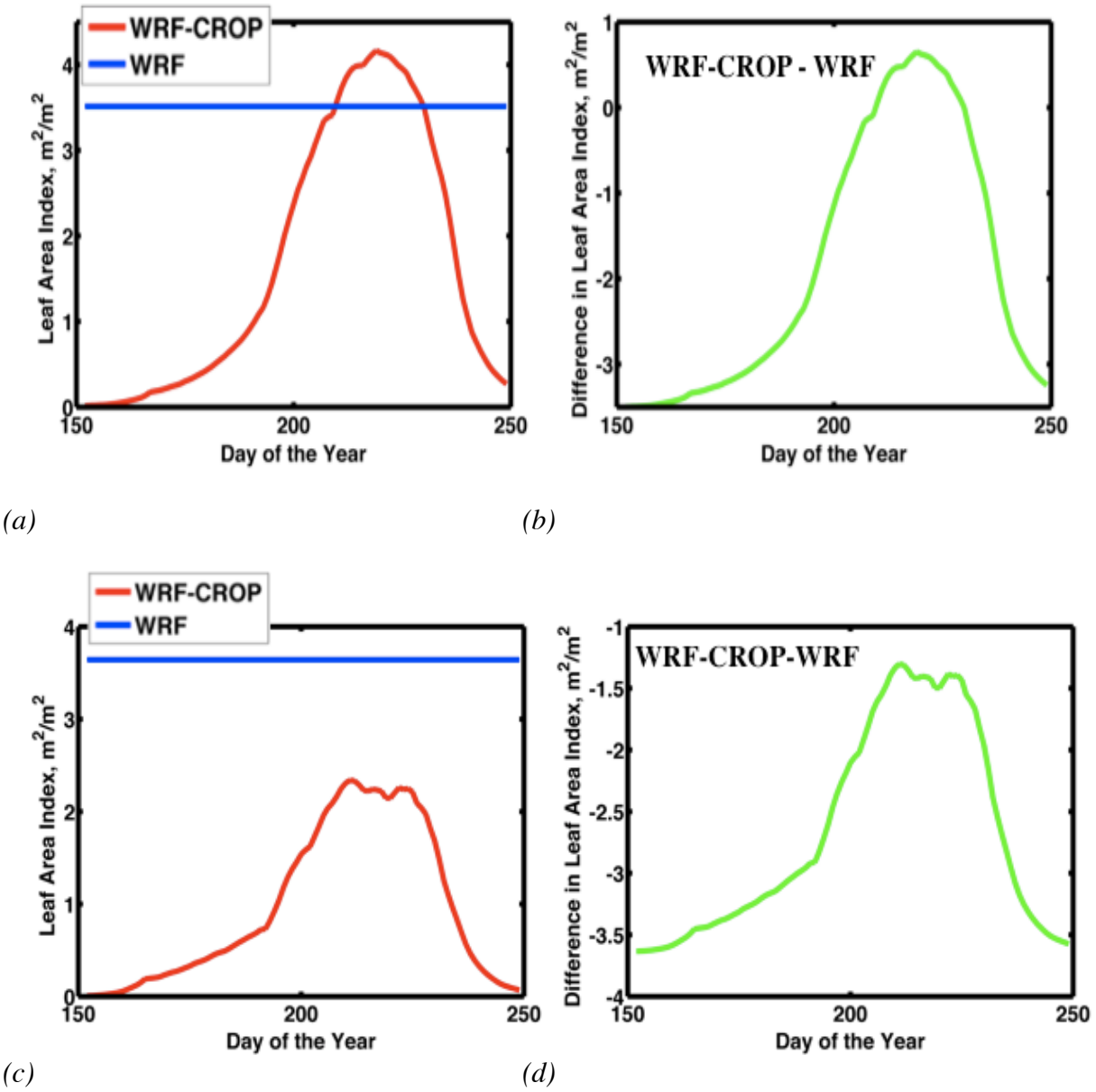

Figure. 4.2 Leaf Area Index simulated by the WRF-CROP model and the WRF model over a) Bondville site c) Nebraska site. Difference in the leaf area index between the WRF-CROP model and the WRF model over b) Bondville site d) Nebraska site.

heat flux also decreased but latent heat flux in the second half of the season was observed to be dominated by the precipitation. In the second half of the season, the precipitation (Figure 4.4) for the WRF-CROP simulations was higher than the WRF simulations over both the sites which replenished the soil moisture (Figure 4.5) more in the WRF-CROP runs as compared to the WRF model runs resulting in a higher latent heat flux for the WRF-CROP coupled model runs than the

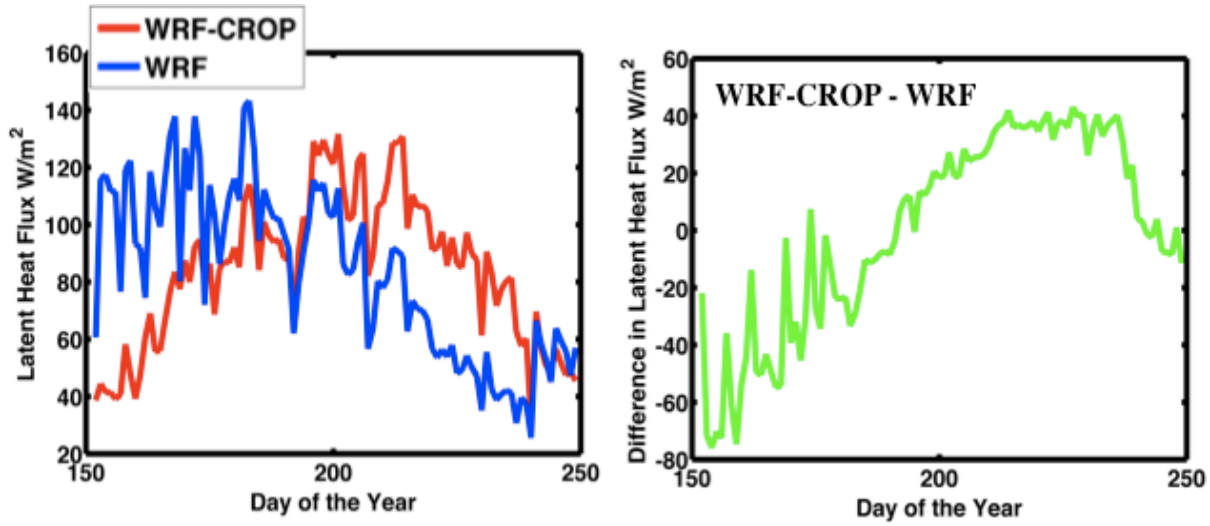

(a) *(b)*

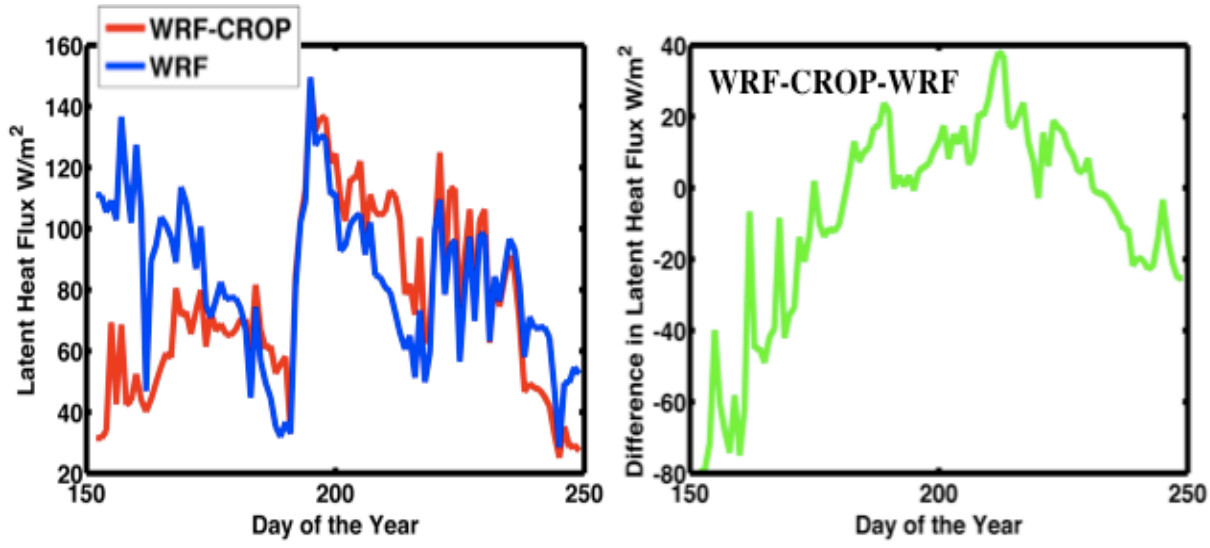

(c) *(d)*

Figure. 4.3 a) Latent heat flux simulated by the WRF-CROP model and the WRF model over a) Bondville site c) Nebraska site. Difference in the latent heat flux between the WRF-CROP model and the WRF model over b) Bondville site d) Nebraska site.

WRF model runs. The sensible heat flux (Figure 4.6) was found to vary inversely with LAI. In the first half of the growing season when LAI in the WRF-CROP simulations was smaller than the WRF simulations, sensible heat flux was higher for the WRF-CROP runs than the WRF runs. As the difference in LAI between the two model runs decreased, the difference in sensible heat

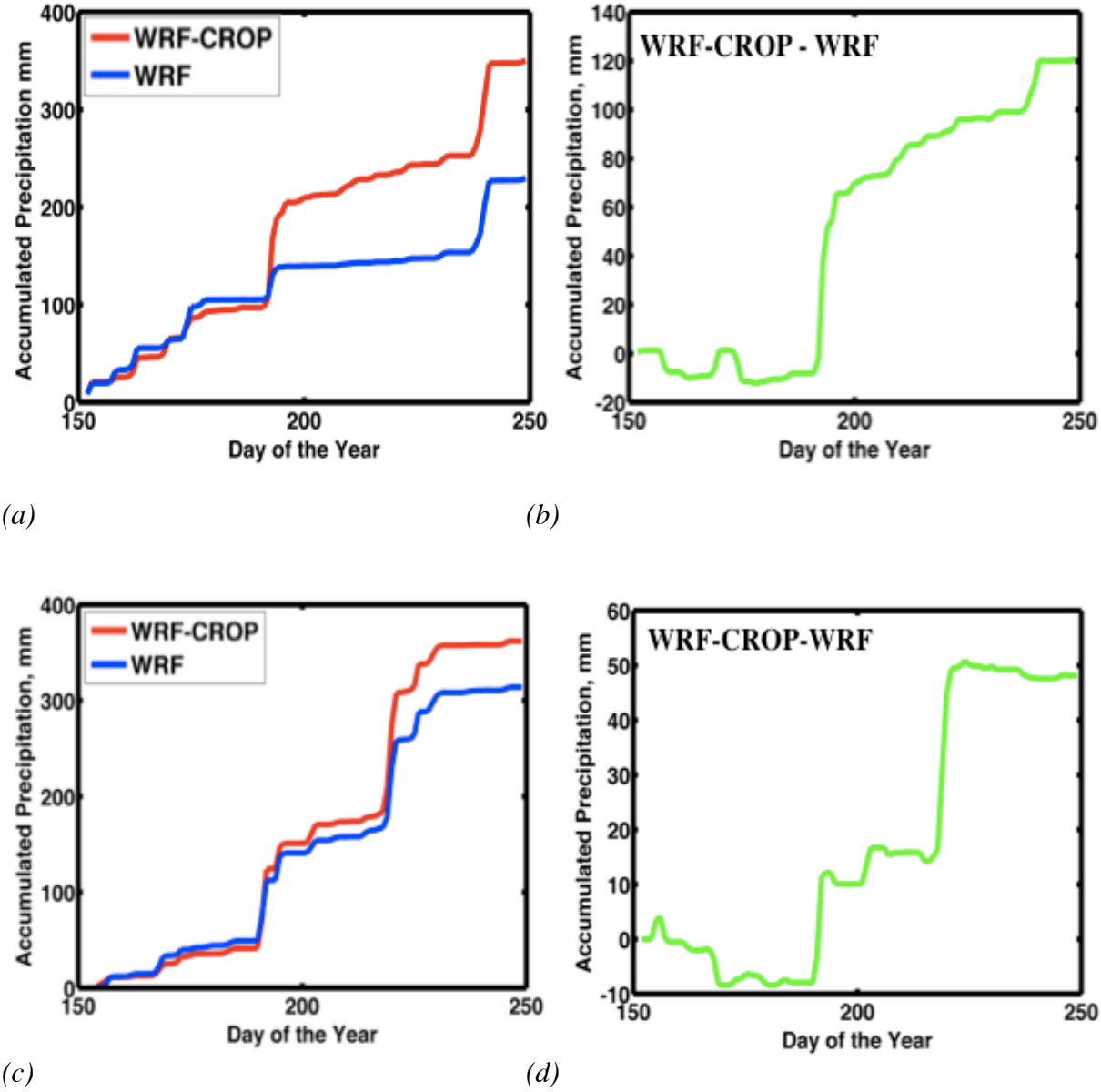

Figure. 4.4 Accumulated precipitation simulated by the WRF-CROP model and the WRF model over a) Bondville site c) Nebraska site. Difference in the accumulated between the WRF-CROP model and the WRF model over c) Bondville site d) Nebraska site.

fluxes between the two also decreased. However, in the second half of the growing season the sensible heat flux was also dominated by precipitation and an increased latent heat flux for WRF-CROP coupled model caused a decrease in sensible heat flux for the coupled model simulations over both the sites. Since the sensible heat flux is the measure of the amount of heat

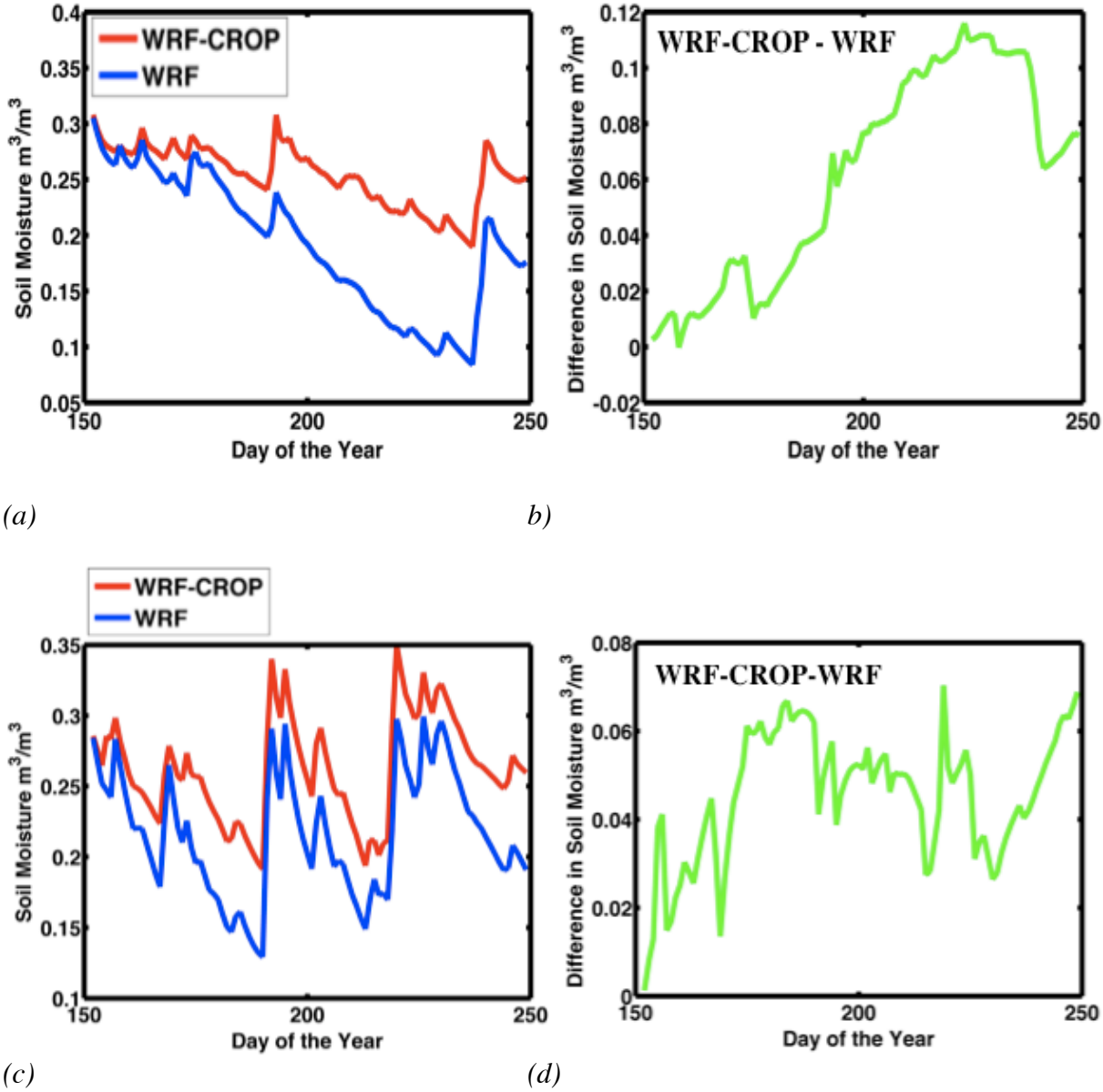

Figure. 4.5 Soil moisture in layer 1 simulated by the WRF-CROP model and the WRF model over a) Bondville site c) Nebraska site. Difference in the soil moisture in layer 1 between the WRF-CROP model and the WRF model over c) Bondville site d) Nebraska site.

energy transferred from the earth's surface to the atmosphere, the near surface air temperature (Figure 4.7) depends on sensible heat flux. In the earlier growth stages, the signal in temperature followed the sensible heat flux. Temperature was higher by 2ºC to 3 ºC for WRF-CROP coupled model simulations as compared to the WRF model simulation over both the sites in the first half of the growing cycle. However, the difference in temperature for the two model simulations

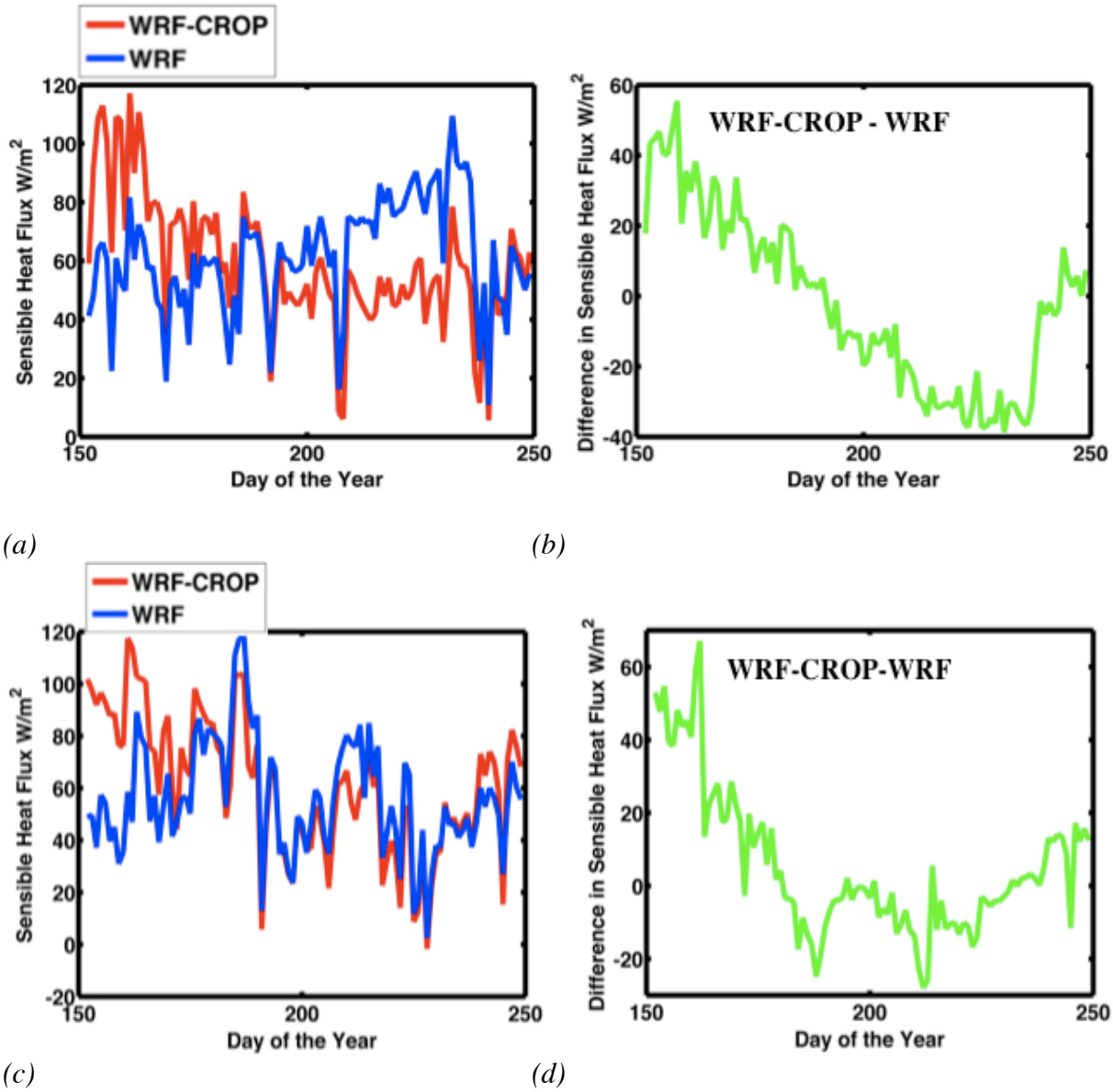

Figure. 4.6 Sensible heat flux simulated by the WRF-CROP model and the WRF model over a) Bondville site c) Nebraska site. Difference in the sensible heat flux between the WRF-CROP model and the WRF model over c) Bondville site d) Nebraska site.

decreased with decreasing difference in LAI. Hence, as the plants grow they exerted a feedback on the temperature, which caused cooling. The temperature in the second half of the cycle was either approximately similar for the two model simulations or WRF-CROP coupled model simulation was a bit cooler. The temperature depends on other factors such as precipitation and

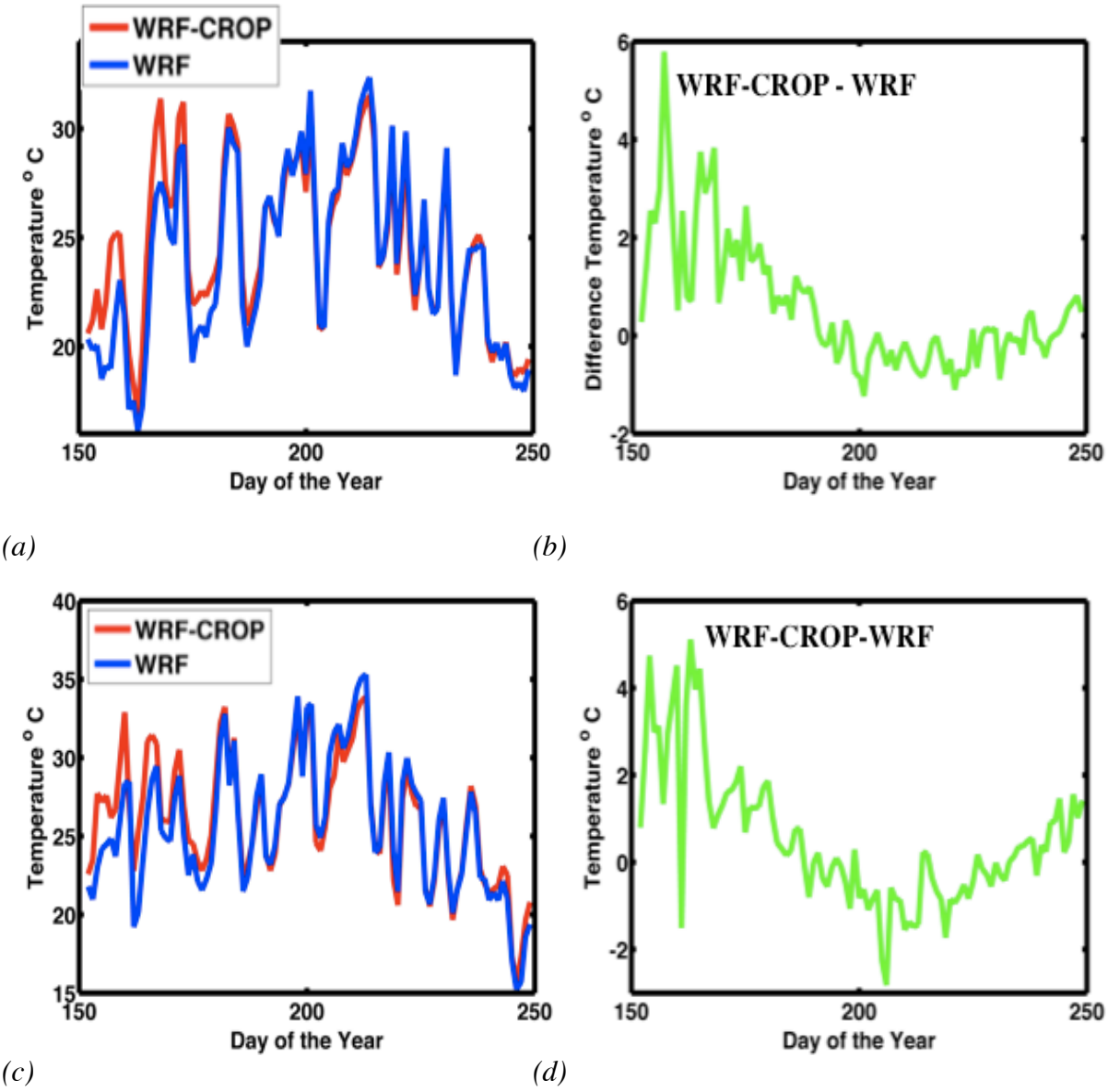

Figure. 4.7 Near surface air temperature simulated by the WRF-CROP model and the WRF model over a) Bondville site c) Nebraska site. Difference in the air temperature between the WRF-CROP model and the WRF model over c) Bondville site d) Nebraska site.

was difficult to understand the effect of dynamic crop growth on these fluxes and hence on the

atmospheric variables. Therefore, to overcome this difficulty and to study the effect of dynamic coupling on the atmosphere another set of experiment was conducted in which precipitation was inhibited. The following section describes the second set of experiments.

4.2.2 Experiment II

In this set of experiments, the microphysics and cumulus scheme was turned off while remaining parameterization was kept similar to the previous set of experiments. This created a

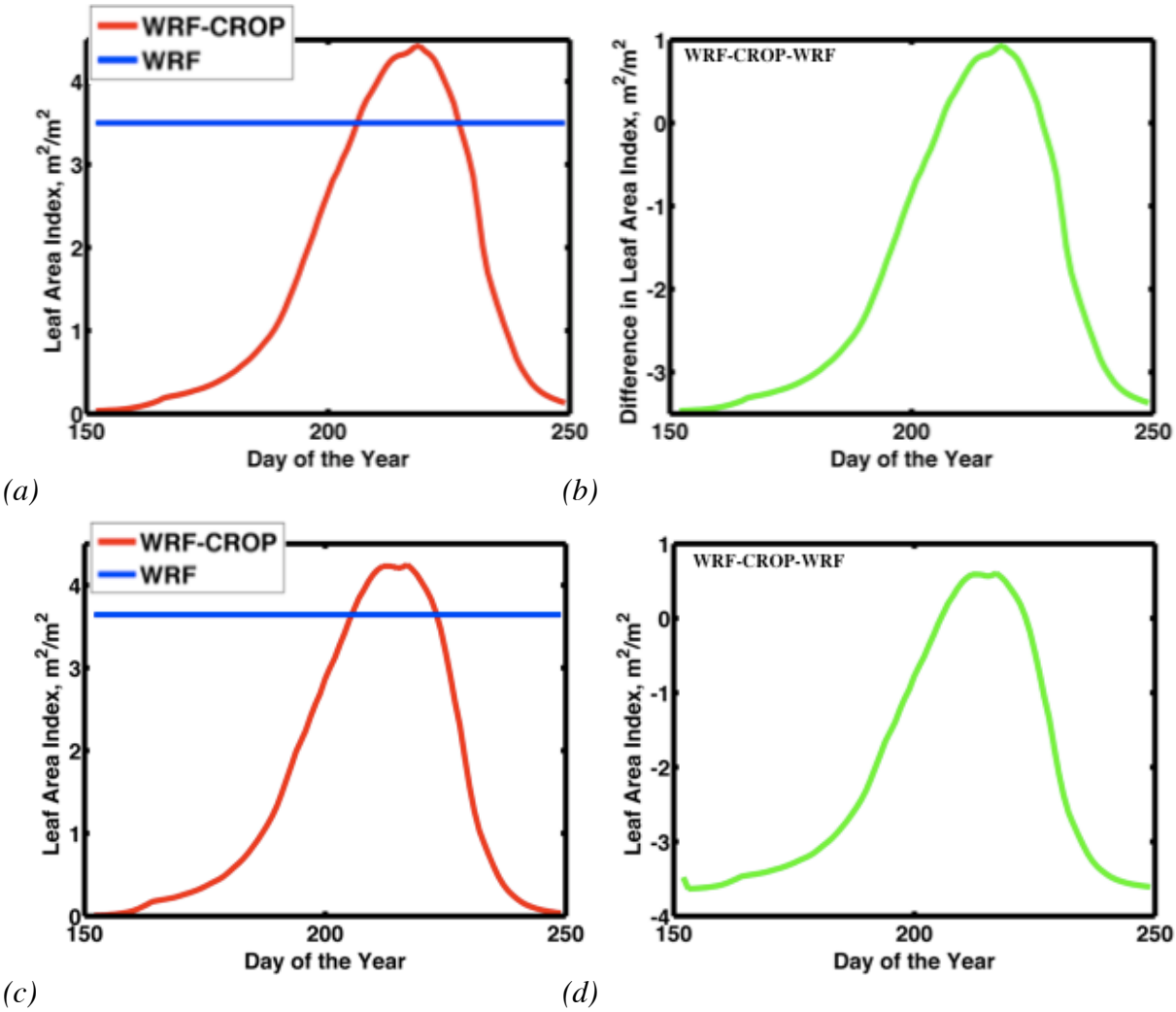

Figure. 4.8 Leaf Area Index simulated by the WRF-CROP model and the WRF model over a) Bondville site c) Nebraska site. Difference in the leaf area index between the WRF-CROP model and the WRF model over b) Bondville site d) Nebraska site.

scenario with no precipitation and no clouds. Constant soil moisture was supplied throughout

the growing season. The presence of sufficient soil moisture throughout the season caused the plants to grow to a peak LAI value of around 4 m^2/m^2 for both the sites in the WRF-CROP coupled model runs while LAI in WRF model runs was constant at around 3.5 m^2/m^2 for both sites (Figure 4.8). Latent heat flux was observed to vary directly with LAI values. In the first half of the growing season, latent heat flux was observed to increase with LAI in the WRF-CROP

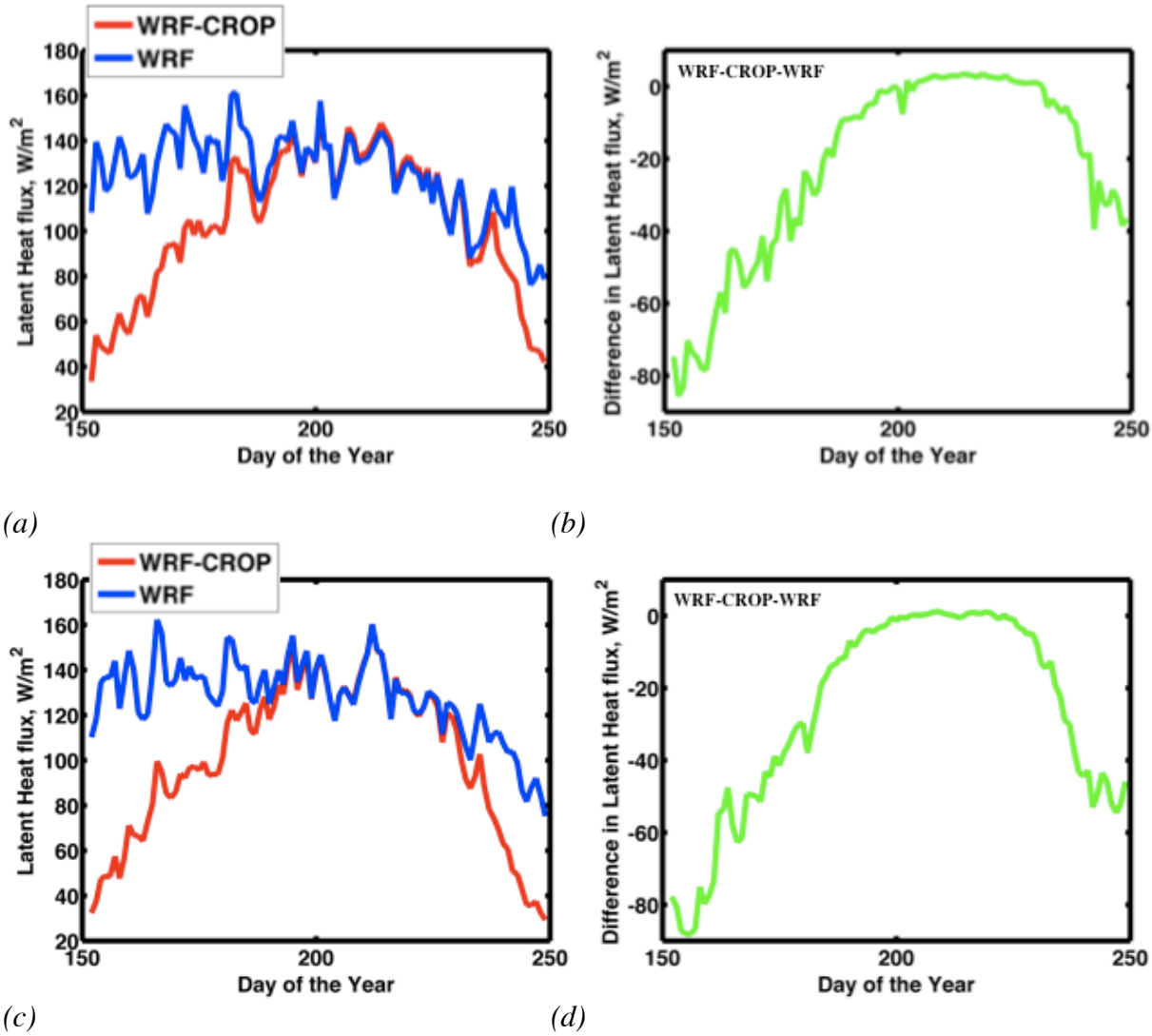

Figure. 4.9 a) Latent heat flux simulated by the WRF-CROP model and the WRF model over a) Bondville site c) Nebraska site. Difference in the latent heat flux between the WRF-CROP model and the WRF model over b) Bondville site d) Nebraska site.

model results while latent heat flux was similar in the WRF model results for both the sites (Figure 4.9). In the second half of the growing season, as the plants start to die latent heat flux was observed to decrease in the WRF-CROP coupled model. The difference between latent heat fluxes for the two model runs (Figure 4.9b and Figure 4.9d) was found to vary directly with the difference between LAIs (Figure 4.8b and Figure 4.8d) between the two model runs. On the

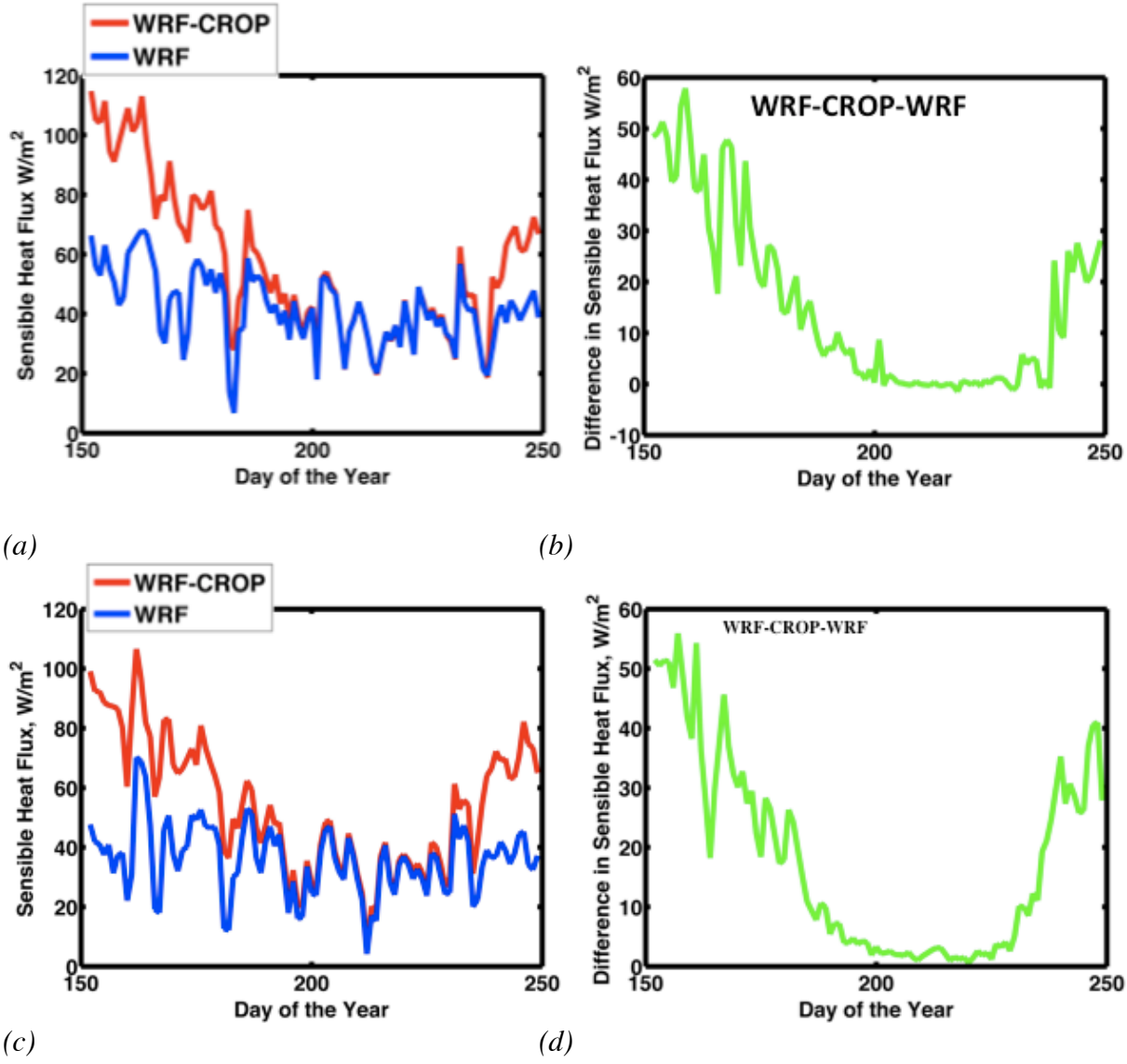

Figure. 4.10 Sensible heat flux simulated by the WRF-CROP model and the WRF model over a) Bondville site c) Nebraska site. Difference in the sensible heat flux between the WRF-CROP model and the WRF model over c) Bondville site d) Nebraska site.

other hand, sensible heat flux (Figure 4.10) varies inversely with LAI. In the beginning, sensible heat flux for WRF-CROP coupled model runs was higher as compared to the WRF model runs. As LAI value increased sensible heat flux reduced over the croplands and in the latter half of growth cycle as plants began to die, LAI reduced and hence sensible heat flux increased. The difference in sensible heat fluxes (Figure 4.9b and Figure 4.9d) between the two model runs was observed to vary inversely with the difference between LAIs (Figure 4.8b and Figure 4.8d) for

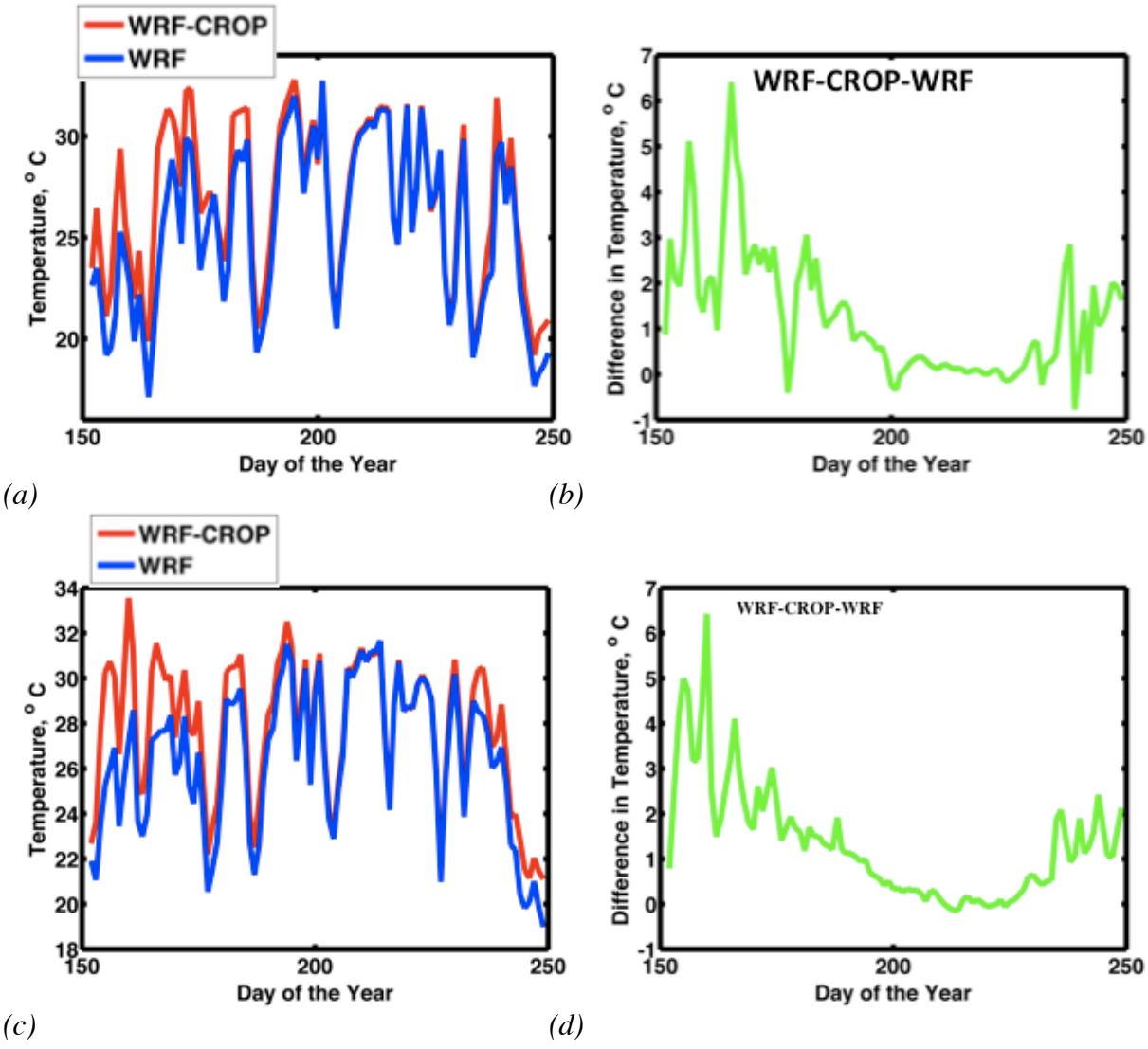

Figure. 4.11 Near surface air temperature simulated by the WRF-CROP model and the WRF model over a) Bondville site c) Nebraska site. Difference in the air temperature between the WRF-CROP model and the WRF model over c) Bondville site d) Nebraska site.

the two model runs. The air temperature over the two sites (Figure 4.11) varied directly with sensible heat fluxes. The WRF-CROP coupled model was warmer in the beginning as compared to the WRF model simulation by an average value of 3ºC. As the growth increased in the WRF-CROP coupled model, it exerted a feedback on the air temperature, which caused a cooling. On the other hand, in latter half of the growing season as the plants begin to die they exerted another opposite feedback on the air temperature, which resulted in warming.

4.3 Conclusion

- The WRF-CROP coupled model was able to simulate leaf area index comparable to the MODIS data over the two sites in the Midwestern United States.
- The comparison of results from two models with constant and dynamic crop growth explained the effect of growth on the atmosphere.
- Latent heat flux was observed to vary directly with LAI. Difference in latent heat flux between the two model runs directly followed the difference in LAI between the two models.
- Sensible heat flux was observed to vary inversely with LAI. Difference in sensible heat flux between the two model runs inversely followed the difference in LAI between the two models.
- The growth was observed to exert a feedback on the air temperature. In the WRF-CROP model, initially when LAI was low, the temperature was higher while as growth increased it exerted a feedback on air temperature by decreasing sensible heat flux and producing cooling. In the second half of growing cycle, as the plants began to die they exerted an opposite feedback on temperature by increasing sensible heat resulting in warming.

CHAPTER 5

CONCLUSION & DISCUSSION

5.1 Conclusion

The crop growth model based on the SUCROS model was used to simulate the crop growth over the Ameriflux soybean site in Nebraska. Sensitivity studies were conducted to understand the forcing-response relationship between the atmosphere and the cropland. It was observed that decreasing temperature over the season reduced the growth in the juvenile stage while increased the growth in the remaining season. However, a minimum temperature threshold of 7ºC was observed and any decrease in temperature beyond 7ºC decreased growth. Increasing temperature increased growth in juvenile stage and reduced growth in the mature stage. Life span of the plants was observed to vary inversely with the near surface air temperature. Decreasing precipitation resulted in a decreased growth due to limited soil moisture supply while increasing precipitation increased growth by making more soil moisture available to the plants. However, any increase in soil moisture above 60% saturation reduced growth. Decrease in incoming shortwave radiation increased growth but any decrease in radiation above 30% reduced growth. Increasing radiation over the entire season reduced growth due to reduced moisture availability. The days when incoming radiation was low, increase in radiation was seen to increase the growth as the effect of increase in photosynthetic radiation dominated over the effect of lower moisture availability. Multi-variable sensitivity study was conducted to study the combined effect of two atmospheric variables at a time. The variables either act synergistically or competitively to effect growth and the net result was a non linear combination of the two forcing.

The crop growth model only simulated forcing-response relationship between the atmosphere and the croplands and was not capable of simulating the feedbacks between the two.

In order to study these atmosphere-croplands feedbacks, a computationally efficient modeling tool known as WRF-CROP coupled model was developed by incorporating a crop growth module derived from SUCROS model into the Weather Research Forecasting model. The WRF-CROP coupled model was successfully able to simulate dynamic crop growth for soybean crops over the two sites in the Mid Western United States. The effect of individual atmospheric variables such as precipitation, radiation and soil moisture on the crop growth was studied by modifying the model parameterization. In the absence of precipitation, a soil water stress situation was created which reduced the crop growth while on supplying constant soil moisture under no precipitation conditions the growth increased. Hence, the crop growth directly varies with the soil moisture. Incoming shortwave radiation plays an important role in the growth by controlling PAR and soil water evaporation. The effect of radiation was studied by comparing the simulations with and without the clouds and difference in LAI for the two runs was found to be small. Near surface air temperature was found to be another important factor that affects growth. The growth was found to vary inversely with the air temperature. Warming was observed to reduce growth while cooling was observed to increase growth.

Finally, the effect of growth on the atmosphere was investigated. The comparison of results from two models with constant and dynamic crop growth explained the effect of growth on the atmosphere. Latent heat flux was observed to vary directly with LAI. Difference in latent heat flux between the two model runs directly followed the difference in LAI between the two models. Sensible heat flux was observed to vary inversely with LAI. Difference in sensible heat flux between the two model runs inversely followed the difference in LAI between the two models. The growth was observed to exert a feedback on the air temperature. In the WRF-CROP model, initially when LAI was low, the temperature was higher while as growth increased it

exerted a feedback on air temperature by decreasing sensible heat flux and producing cooling. In the second half of growing cycle, as the plants began to die they exerted an opposite feedback on temperature by increasing sensible heat resulting in warming.

It was observed that the crop growth varies with changes in atmospheric variables such as precipitation, incoming shortwave radiation and temperature. At the same time, the crop growth was observed to influence latent heat flux, sensible heat flux and near surface air temperature by exerting a feedback on the atmosphere.

5.2 Discussion

This study focuses on the cropland-atmosphere interactions i.e., the effect of atmosphere on the crop growth and the feedback exerted by growth on the atmosphere. The effect of various atmospheric variables on the crop growth was observed using both the standalone crop growth model and WRF-CROP coupled model. The WRF-CROP coupled model incorporates dynamic crop growth and hence it is also capable of simulating the feedback of growth on the atmosphere. However, as mentioned in the previous section, the effect of growth was observed on the latent heat flux, sensible heat flux, and near surface air temperature. The effect of growth on other variables such as precipitation was not investigated in this study. In future, I intend to enhance this study by exploring the feedback of crop growth on precipitation. This aim can be achieved by obtaining a robust precipitation signal using an ensemble of simulations from both the models: WRF model with constant vegetation and WRF-CROP model with dynamic vegetation. A comparison of these two model results will provide a better understanding of the effect of growth on the precipitation.

At present, the WRF-CROP coupled model is capable of simulating dynamic growth for only one crop type. This limits the applicability of the model over multiple crop fields. I plan to

extend the capability of WRF-CROP coupled model by incorporating multiple crop types in the model. This will allow us to apply the model over an area with different crop types and also make the WRF-CROP model an important tool to study the effect of landuse/land cover change on the local climate.

REFERENCES

Arora, V. (2002). Modeling vegetation as a dynamic component in soil-vegetation-atmosphere transfer schemes and hydrological models. *Reviews of Geophysics, 40*(2), 1006. doi: 10.1029/2001RG000103

Betts, R. (2005). Integrated approaches to climate-crop modelling: Needs and challenges. *Philosophical Transactions of the Royal Society B-Biological Sciences, 360*(1463), 2049-2065. doi: 10.1098/rstb.2005.1739

Bonan, G., Levis, S., Sitch, S., Vertenstein, M., & Oleson, K. (2003). A dynamic global vegetation model for use with climate models: Concepts and description of simulated vegetation dynamics. *Global Change Biology, 9*(11), 1543-1566. doi: 10.1046/j.1365-2486.2003.00681.x

Brunsell, N. A., & Anderson, M. C. (2011). Characterizing the multi-scale spatial structure of remotely sensed evapotranspiration with information theory. *Biogeosciences, 8*(8), 2269-2280. doi: 10.5194/bg-8-2269-2011

Chen, F., & Xie, Z. (2011). Effects of crop growth and development on land surface fluxes. *Advances in Atmospheric Sciences, 28*(4), 927-944. doi: 10.1007/s00376-010-0105-1

Cox, P. M. (2001). Description of the TRIFFID dynamic global vegetation model. Technical Note 24, Hadley Centre, Met Office, London Road, Bracknell, Berks, RG122SY, UK.

Dan, L., Ji, J., & Li, Y. (2005). Climatic and biological simulations in a two-way coupled atmosphere-biosphere model (CABM). *Global and Planetary Change, 47*(2-4), 153-169. doi: 10.1016/j.gloplacha.2004.10.019

Foley, J., Levis, S., Prentice, I., Pollard, D., & Thompson, S. (1998). Coupling dynamic models of climate and vegetation. *Global Change Biology, 4*(5), 561-579. doi: 10.1046/j.1365-2486.1998.t01-1-00168.x

Goudriaan, J., & H. H. van Laar (1994), Modelling Potential Crop Growth Processes, 2nd ed., 274 pp., Kluwer, Dordrecht, Netherlands.

Henderson-Sellers, A., & Mcguffie, K. (1995). Global climate models and dynamic vegetation changes. *Global Change Biology, 1*(1), 63-75. doi: 10.1111/j.1365-2486.1995.tb00007.x

Ji, J. (1995). A climate-vegetation interaction model: Simulating physical and biological processes at the surface. *Journal of Biogeography, 22*(2-3), 445-451. doi: 10.2307/2845941

Jiang, X., Niu, G., & Yang, Z. (2009). Impacts of vegetation and groundwater dynamics on warm season precipitation over the Central United States. *Journal of Geophysical Research-Atmospheres, 114*, D06109. doi: 10.1029/2008JD010756

Krinner, G., Viovy, N., de Noblet-Ducoudre, N., Ogee, J., Polcher, J., Friedlingstein, P., .Prentice, I. (2005). A dynamic global vegetation model for studies of the coupled atmosphere-biosphere system. *Global Biogeochemical Cycles, 19*(1), GB1015. doi: 10.1029/2003GB002199

Kumar, A., Chen, F., Niyogi, D., Alfieri, J. G., Ek, M., & Mitchell, K. (2011). Evaluation of a photosynthesis-based canopy resistance formulation in the noah land-surface model. *Boundary-Layer Meteorology, 138*(2), 263-284. doi: 10.1007/s10546-010-9559-z

Lu, L., Pielke, R., Liston, G., Parton, W., Ojima, D., & Hartman, M. (2001). Implementation of a two-way interactive atmospheric and ecological model and its application to the central united states. *Journal of Climate, 14*(5), 900-919. doi: 10.1175/1520-0442(2001)014<0900:IOATWI>2.0.CO;2

Murata, N. (1992) Research in photosynthesis: proceedings of the IXth International Congress on Photosynthesis, Nagoya, Japan, August 30- September 4.

Osborne, T. M., Lawrence, D. M., Challinor, A. J., Slingo, J. M., & Wheeler, T. R. (2007). Development and assessment of a coupled crop-climate model. *Global Change Biology, 13*(1), 169-183. doi: 10.1111/j.1365-2486.2006.01274.x

Penning de Vries, F.W.T. & H.H. van Laar. (1982). Simulation of plant growth and crop production. Simulation Monographs, Pudoc, Wageningen, 308.

Penning de Vries, F.W.T., D.M. Jansen, H.F.M. ten Berge & A. Bakema. (1989). Simulation of ecophysiological processes of growth of several annual crops. Simulation Monographs 29, Pudoc, Wageningen, 271.

Sato, H., Itoh, A., & Kohyama, T. (2007). SEIB-DGVM: A new dynamic global vegetation model using a spatially explicit individual-based approach. *Ecological Modelling, 200*(3-4), 279-307. doi: 10.1016/j.ecolmodel.2006.09.006

Setiyono, T. D., Weiss, A., Specht, J. E., Cassman, K. G., & Dobermann, A. (2008). Leaf area index simulation in soybean grown under near-optimal conditions. *Agronomy -- Faculty Publications,* 113. doi:10.1016/j.fcr.2008.03.005

Shin, D., Bellow, J., Larow, T., Cocke, S., & O'Brien, J. (2006). The role of an advanced land model in seasonal dynamical downscaling for crop model application. *Journal of Applied Meteorology and Climatology, 45*(5), 686-701. doi: 10.1175/JAM2366.1

Skamarock, W., Klemp, J.B., Dudhia, J., Gill, D.O., Barker, D., Duda, M.G., Huang, X.-Y., Wang, W., & Powers, J.G., (2008). A Description of the Advanced Research WRF Version 3. Technical Note. NCAR/TN–475+STR, National Center for Atmospheric Research, Boulder, Colorado.

Snyder, P., Foley, J., Hitchman, M., & Delire, C. (2004). Analyzing the effects of complete tropical forest removal on the regional climate using a detailed three-dimensional energy budget: An application to Africa. *Journal of Geophysical Research-Atmospheres, 109*(D21), D21102. doi: 10.1029/2003JD004462

Tsvetsinskaya, E., Mearns, L., & Easterling, W. (2001). Investigating the effect of seasonal plant growth and development in three-dimensional atmospheric simulations. part I: Simulation of surface fluxes over the growing season. *Journal of Climate, 14*(5), 692-709. doi: 10.1175/1520-0442(2001)014<0692:ITEOSP>2.0.CO;2

Van den Hoof, C., Hanert, E., & Vidale, P. L. (2011). Simulating dynamic crop growth with an adapted land surface model - JULES-SUCROS: Model development and validation. *Agricultural and Forest Meteorology, 151*(2), 137-153. doi: 10.1016/j.agrformet.2010.09.011

Zeng, H., Wang, Z., Ji, J., & Wu, G. (2008). An updated coupled model for land-atmosphere interaction. part I: Simulations of physical processes. *Advances in Atmospheric Sciences, 25*(4), 619-631. doi: 10.1007/s00376-008-0619-y